

THESIS / THÈSE

MASTER IN BIOCHEMISTRY AND MOLECULAR AND CELL BIOLOGY RESEARCH FOCUS

Study of the implication of reactive oxygen species in *Caulobacter crescentus* copper-induced negative chemotaxis system

Lamot, Thomas

Award date:
2019

Awarding institution:
University of Namur

[Link to publication](#)

General rights

Copyright and moral rights for the publications made accessible in the public portal are retained by the authors and/or other copyright owners and it is a condition of accessing publications that users recognise and abide by the legal requirements associated with these rights.

- Users may download and print one copy of any publication from the public portal for the purpose of private study or research.
- You may not further distribute the material or use it for any profit-making activity or commercial gain
- You may freely distribute the URL identifying the publication in the public portal ?

Take down policy

If you believe that this document breaches copyright please contact us providing details, and we will remove access to the work immediately and investigate your claim.



Faculté des Sciences

**STUDY OF THE IMPLICATION OF REACTIVE OXYGEN SPECIES IN *CAULOBACTER
CRESCENTUS* COPPER-INDUCED NEGATIVE CHEMOTAXIS SYSTEM**

**Mémoire présenté pour l'obtention
du grade académique de master 120 en biochimie et biologie moléculaire et cellulaire**

Thomas LAMOT

Janvier 2019

Université de Namur
FACULTE DES SCIENCES
Secrétariat du Département de Biologie
Rue de Bruxelles 61 - 5000 NAMUR
Téléphone: + 32(0)81.72.44.18 - Téléfax: + 32(0)81.72.44.20
E-mail: joelle.jonet@unamur.be - <http://www.unamur.be>

Étude de l'implication des espèces réactives de l'oxygène dans la réponse chimiotactique négative de *Caulobacter crescentus*

LAMOT Thomas

Résumé

Le cuivre est un métal lourd bien connu pour être toxique à forte dose chez la plupart des organismes. Récemment, la réponse unique face au cuivre de la bactérie dimorphique *Caulobacter crescentus* a été décrite. Là où la cellule pédonculée expulse le cuivre de son périplasme, la cellule flagellée engage une réponse de fuite vers un environnement sans cuivre. L'hypothèse actuelle est que cette réponse de fuite est médiée par un système de chimiotactisme. Cependant, le cuivre est capable d'induire un stress oxydatif *in vitro*. De ce fait, deux hypothèses non-exclusives sont possibles : les chémorécepteurs sont soit capables de sentir directement le cuivre, soit des espèces réactives de l'oxygène générées par le cuivre.

La première partie de cette étude avait pour but de déterminer si le cuivre est capable d'impacter l'équilibre redox de *C. crescentus* en générant des espèces réactives de l'oxygène. Des analyses par fluorimétrie et microscopie à fluorescence en utilisant une sonde YFP sensible à l'état redox ont permis de montrer que le cuivre est capable d'altérer la balance glutathion oxydé/réduit en faveur du glutathion oxydé.

La seconde partie avait pour but de tester le chimiotactisme envers l'H₂O₂ et le paraquat dichlorure de mutants KO pour des gènes candidats impliqués dans la perception du cuivre. Étonnement cela a permis l'identification de potentiels candidats pour la perception de l'O₂. Finalement la délétion de *yaaA*, une protéine potentiellement impliquée dans la résistance à l'H₂O₂ semble augmenter la fuite à l'H₂O₂ de *C. crescentus*.

Mémoire de master 120 en biochimie et biologie moléculaire et cellulaire

Janvier 2019

Promoteur: J.-Y. Matroule

Université de Namur
FACULTE DES SCIENCES
Secrétariat du Département de Biologie
Rue de Bruxelles 61 - 5000 NAMUR
Téléphone: + 32(0)81.72.44.18 - Téléfax: + 32(0)81.72.44.20
E-mail: joelle.jonet@unamur.be - <http://www.unamur.be>

Study of the implication of reactive oxygen species in *Caulobacter crescentus* copper-induced negative chemotaxis system

LAMOT Thomas

Summary

Copper is a heavy metal which is well-known to be toxic at high doses for most organisms. Recently, an original defense strategy has been described in the dimorphic bacteria *Caulobacter crescentus* when exposed to copper stress. Whereas the stalked cells expel copper from their cytoplasm, the swarmer cells accumulate copper and engage readily a flight response to find a copper-free environment. This flight response is likely mediated by a chemotaxis system. However, as copper is known to induce oxidative stress *in vitro*, it is not clear whether the cues sensed by the chemoreceptors are either copper or copper-induced reactive oxygen species.

The first part of this study aimed to determine whether copper is able to impact the redox balance of *C. crescentus* by generating reactive oxygen species. Using a redox-sensitive YFP as a reporter of the *in vivo* glutathione redox state, fluorometry analysis and fluorescence microscopy showed that copper is able to shift the normal oxidized/reduced glutathione equilibrium toward oxidized glutathione.

On the second part, chemotaxis of KO mutants of candidate genes for copper sensing was tested toward H₂O₂ and paraquat dichloride. Interestingly, some candidates for O₂ sensing were also described. Finally, a KO mutant of *yaaA*, a protein thought to be involved in H₂O₂ resistance, was found to display an increased H₂O₂ flight.

Mémoire de master 120 en biochimie et biologie moléculaire et cellulaire

Janvier 2019

Promoteur: J.-Y. Matroule

AKNOWLEDGMENTS

Mes premiers remerciements vont à Jean-Yves Matroule, mon promoteur, pour avoir pu réaliser mon mémoire au sein de son équipe, son optimisme sans faille, ses précieux conseils, son temps passé à guider mon mémoire et corriger ma rédaction ainsi son grand calme surtout lors d'accrochages au détour d'un couloir où, heureusement, les pertes n'auront été que caféinées.

Un tout grand merci à Gwen, ma tutrice, pour son immense patience envers moi (Tu as dû en avoir beaucoup besoin par moment !) mais également pour m'avoir transmis sa passion pour la science, de m'avoir montré que la microscopie c'est super cool même si le microscope n'est pas toujours droit (un comble pour un inversé !) et de m'avoir mis quelques coups de pied au c** quand j'en avait besoin.

Merci au reste de la team BEAR, Seb, Françoise et Pauline. Pour leur disponibilité et leur bonne humeur quotidienne. Seb, merci pour ton coup de main avec la bioinfo et de m'avoir expliqué certaines manips quand Gwen était en vacances. Pauline, merci de tes conseils précieux, j'ai appris un peu plus écolo grâce à toi ! Merci Françoise d'avoir pris du temps à chaque fois que j'arrivais avec un problème (Françoise... la balance fait un truc pas normal...)

Merci à Angy qui a pris de son temps lorsque j'avais quelques questions ou que le microscope faisait des caprices en l'absence de Gwen, d'avoir supporté mon humour de très haut niveau qui m'a valu quelques points en moins avant même que tu aies mon mémoire en main (D'ailleurs est-ce que ça suffit pour repasser de -43 à -42 ?).

Merci à Clara pour le temps qu'elle a passé avec moi à essayer de faire marcher ma manip au fluorimètre et sa théorie farfelue qui s'est avérée être correcte.

Merci aux mémos et aux stagiaires, Boutaina, Mel et Antoine, qu'ils aient partagé le même bureau ou qu'ils soient les voisins du GéMo. Merci à Ysa, camarade du cours d'anglais on se sera bien marré avec nos expériences avec des chaussettes ! Merci à Fx, qui m'a fait découvrir l'impro qui m'a permis de décompresser chaque lundi soir depuis l'an passé (Big up à l'Impronam) et qui est toujours présent pour des discussions plus ou moins scientifiques ! Enfin, merci à Eme, d'avoir été là, que ce soit dans des moments de stress de joie ou de doute, pour les conseils d'organisation (Je promets de les appliquer à l'avenir) et pour toujours tenir au courant des tes besoins en sommeil (« J'veux faire dodo ! »). Le bureau mémo aurait été vide sans toi (non mais littéralement, je me serais retrouvé tout seul !).

Merci au reste de l'URBM, pour leur accueil et leur bonne humeur quotidienne.

Un grand merci au GéMo pour l'organisation hebdomadaire de la beer hour.

Merci à ma famille et à toutes les personnes qui ont eu la joie de prendre le train avec moi (Je pense que vous pourriez présenter ce mémoire tellement j'ai dû vous ennuyer avec mes Caulos).

Finalement merci aux membres de mon jury pour avoir consacré de leur temps pour lire, évaluer et critiquer ce travail.

“ *On découvre de l'ordre
dans certains désordres* ”
Victor Cherbuliez

TABLE OF CONTENTS

| | |
|---|----|
| Résumé..... | 2 |
| Summary | 3 |
| Aknowledgments..... | 4 |
| Table of contents | 6 |
| Introduction | 7 |
| 1. Heavy metal stress..... | 7 |
| 2. Cu the double-edged element..... | 7 |
| 2.1. The origin of Cu | 7 |
| 2.2. Necessity | 7 |
| 2.3. Toxicity | 7 |
| 2.4. Defenses against Cu | 8 |
| 3. Oxidative stress | 9 |
| 4. Chemotaxis..... | 19 |
| 4.1. Movements | 19 |
| 4.2. Signal sensing..... | 19 |
| 4.3. Signal transduction..... | 11 |
| 4.4. Adaptative system | 21 |
| 4.5. Sensory repertoire | 12 |
| 5. <i>Caulobacter crescentus</i> | 12 |
| 5.1. Redox state & Cell cycle..... | 12 |
| 5.2. Response to Cu stress..... | 14 |
| 5.2.1. Chemotaxis..... | 14 |
| 5.3. Defenses against oxidative stress | 15 |
| Objectives..... | 19 |
| Result & Discussion | 21 |
| 1. Assessment of <i>in vivo</i> production of Cu-induced ROS..... | 21 |
| 2. Impact of ROS on <i>C. crescentus</i> chemotaxis..... | 26 |
| 3. Issues and potential improvements of LCI..... | 28 |
| Conclusion & Perspectives..... | 29 |
| Methods..... | 30 |
| References | 32 |

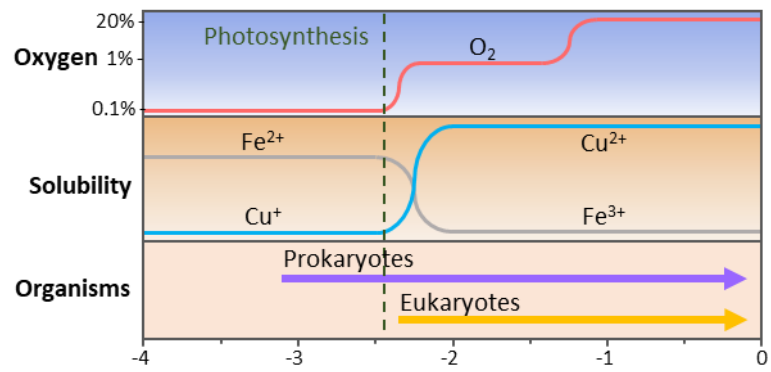


Figure 1: Evolution over time of atmospheric oxygen level; solubility, bioavailability and oxidation state of copper and iron; apparition of prokaryotic, eukaryotic organisms and apparition of photosynthesis (adapted from Solioz, 2018)

INTRODUCTION

1. Heavy metal stress

Heavy metals like copper (Cu), cadmium, lead, zinc (Zn) or uranium always existed in relatively scarce quantities in soils and waters. However, with the rise of modern technologies, the extensive use of those metals in anthropogenic activities such as the agriculture and the industry led to huge increases in heavy metals concentration in the environment. As those are not easily detoxified, they tend to accumulate even more, leading to a heavy metal pollution. This causes huge impacts at every level, from changes in the composition of microbial communities to health issues in humans through the bioaccumulation of such metals. So researches on how some organisms are able to cope with heavy metal stress became more and more important (Ahemad, 2012; Etesami, 2018).

2. Cu the double-edged element

Cu is a transition metal often found in two main forms: an oxidized form (Cu^{2+}) and a reduced form (Cu^+). Sometimes, Cu can also be found on the scarcer more oxidized forms Cu^{3+} and Cu^{4+} . One of the main differences between Cu^+ and Cu^{2+} for biological processes is that Cu^{2+} is soluble in water making it more bioavailable than Cu^+ . Cu^{2+} is the predominant Cu ionic form found in the oxidant periplasm. However, Cu^{2+} is likely reduced into Cu^+ when entering the more reducing cytoplasm (Solioz, 2018).

2.1. The origin of Cu

Three billion years ago, the first photosynthetic organisms appeared and the O_2 generated by their photosynthesis modified the redox conditions at the cell surface, turning insoluble Cu^+ into soluble Cu^{2+} (Figure 1). Concomitantly, soluble Fe^{2+} was oxidized into Fe^{3+} , thereby reducing its solubility and its bioavailability. When most of the Cu and Fe were oxidized, the O_2 atmospheric levels were allowed to rise up to the current level of 21%. This rising of O_2 levels created new stresses, the oxidative stresses, and the need for new defenses and strategies to face them (Solioz, 2018).

2.2. Necessity

At low doses, Cu is an essential element for a wide range of biological processes. It is needed for the activity and stability of a lot of proteins and complexes *e.g.* the Cu-Zn superoxide dismutase; the hemocyanin, a respiratory pigment often found in arthropods and mollusks; or even the complex IV of the electron transport chain (Bondarczuk and Piotrowska-Seget, 2013; Solioz, 2018). Some species are able, in case of Cu deficiency, to synthesize chalkophores. Chalkophores are the Cu pendant of siderophore, they are molecules able to chelate Cu to improve its import in the cell although some have others functions such a signaling factors or superoxide dismutase activity (Kenney and Rosenzweig, 2018).

2.3. Toxicity

However, at high doses, Cu can become toxic. Indeed, Cu is able to take the place of other metals in metalloproteins. A well-known example is the displacement of iron-sulfur (Fe-S)

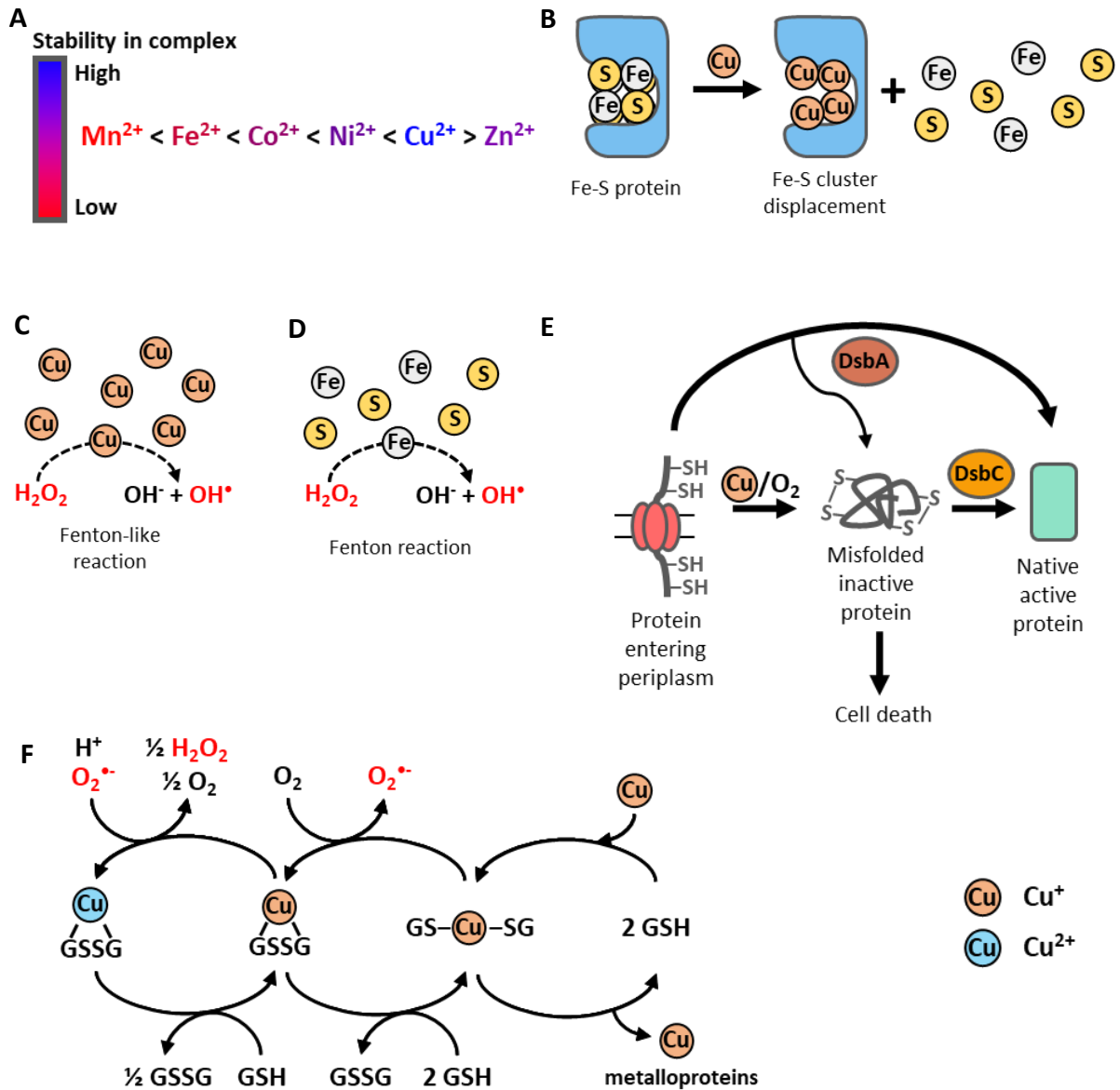


Figure 2: Toxicity mechanisms of copper. A) Order of stability of divalent metals in complexes as described by Irving and Williams. B) Copper taking place of a iron-sulfur cluster. C) Formation of copper-induced non native disulfide bond on periplasmic protein. D) ROS formation through Fenton-like reaction catalyzed by copper ions. E) ROS formation through Fenton reaction catalyzed by iron ions displaced by copper ions (see panel A). F) ROS generated by copper sequestration through the glutathione redox buffer.

cluster in Fe-S proteins as it is thought to be the main source of Cu toxicity (Macomber and Imlay, 2009) (Figure 2B). A lot of these proteins are involved in essential pathways such as the aconitase in the TCA cycle. These displacements are mostly due to the high stability of Cu^{2+} in complexes as shown by the Irving-Williams series (Figure 2A) and explained by the Hard-Soft Acid-Base (HSAB) concept of Pearson. The Irving-Williams series is a data collection of the stability of complexes formed by bivalent ions of the first row of transition metals. Irving and Williams observed that in those kinds of complexes, the ones formed with Cu^{2+} are always the most stables (H. Irving and R. J. P. Williams, 1953; Solioz, 2018) (Figure 2A). The HSAB principle shows that hard acids and soft acids tend to better react with hard bases and soft bases, respectively. Cu^{2+} is an intermediate acid but reacts easily with soft bases like thiols. In the HSAB principle, Cu^+ , the Cu form that is mostly found in the cytoplasmic space, is characterized as softer than Cu^{2+} and the other metals like Fe^{2+} . In this case, it is not surprising to see Cu^+ , and sometimes Cu^{2+} , compete for the native binding sites of the other metals in metalloproteins.

Cu might also be able to trigger non-native disulfide bonds formation on periplasmic proteins (Figure 2E). Indeed, under normal conditions, the thiol-disulfide oxidoreductase DsbA catalyzes the correct formation of disulfide bonds in *E. coli* periplasm. However, upon incorrect disulfide bond formation, the main disulfide isomerase DsbC will correct the misfolded proteins. An *E. coli* strain lacking *dsbC* was found to be more sensitive to Cu. Accordingly, Cu was shown to form disulfide bonds in some periplasmic proteins *in vivo* and to form non-native intramolecular disulfide bonds in RNaseA *in vitro*, leading to its inactivation. RNase A activity was restored with the addition of DsbC, further supporting the hypothesis (Hiniker *et al.*, 2005).

Finally, Cu might be able to generate an oxidative stress by the production of reactive oxygen species (ROS) like superoxide anion ($\text{O}_2^{\cdot-}$), hydroxyl radical (HO^{\cdot}) or hydrogen peroxide (H_2O_2) by either a Fenton like reaction-mediated (Figure 2C), a Fenton reaction mediated by the Fe released from the Fe-S clusters (Figure 2D), or by its sequestration by the glutathione redox buffer (Figure 2F) (Freedman *et al.*, 1989; Nies and Herzberg, 2013; Solioz, 2018). However, the *in vivo* relevance of such an oxidative stress is still not clear. It has been shown that Cu does not seem to generate DNA damages in *E. coli* as it would be the case with an oxidative stress (Macomber *et al.*, 2007). However, as most of the Cu is localized in the periplasm, this could explain the absence of DNA damages as any ROS generated by Cu would react before reaching the cytoplasm (Chaturvedi and Henderson, 2014). Still, even if the level of ROS produced are not enough to generate a proper stress it does not mean that they cannot be sensed by the bacteria.

2.4. Defenses against Cu

Bacteria have developed multiple strategies to protect themselves against Cu stress.

The first line of defenses in *E. coli* is the Cu efflux (Cue) system (Figure 3) that mainly acts when the cytoplasmic Cu levels are still low. This system mainly relies on CueR that is able to regulate the expression of the efflux pump *copA* and the multi-copper oxidase (MCO) *cueO*. CopA transport Cu^+ ions from the cytoplasm to the periplasm where they are detoxified into the Cu^{2+} form by CueO (Bondarczuk and Piotrowska-Seget, 2013; Hobman and Crossman, 2015; Ladomersky and Petris, 2015; Solioz, 2018).

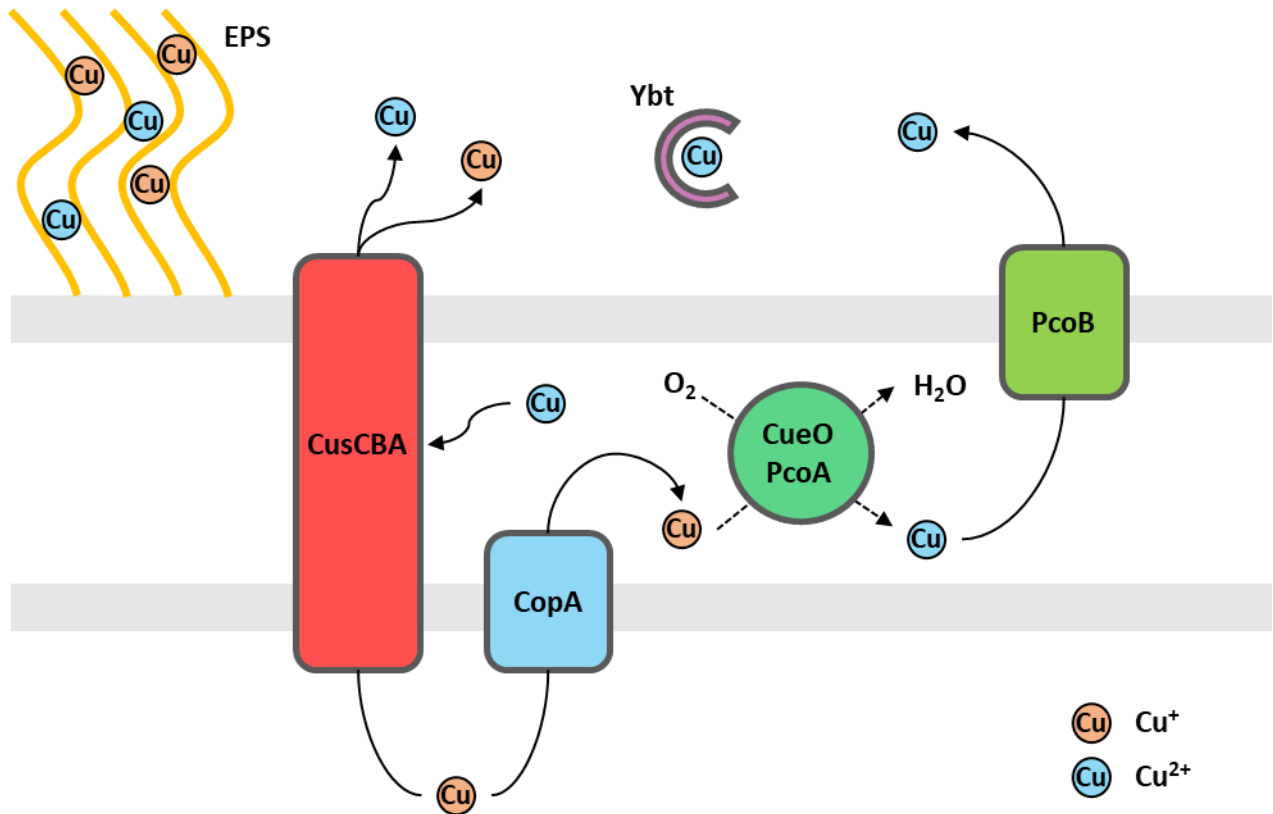


Figure 3: Overview of bacterial defenses against copper stress. Cytoplasmic Cu⁺ is expelled from the cytoplasm by efflux pumps like CusCBA or CopA. Cu⁺ can also be detoxified into Cu²⁺ by multicopper oxidases like CueO or PcoA. The Cu²⁺ ions can then be expelled from the cytoplasm by efflux pump like CusCBA or PcoB. Extracellular Cu ions can also be sequestered by EPS or siderophore like the Ybt. EPS: exopolysaccharide. Ybt: Yersiniabactin. Cus: Cu sensing. Cue: Cu efflux. Pco: Plasmid borne Cu resistance.

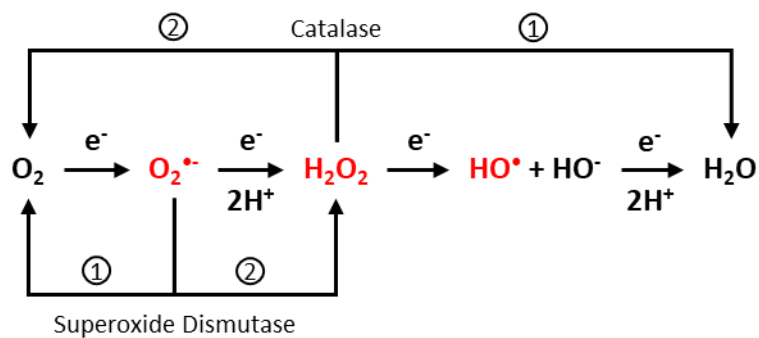
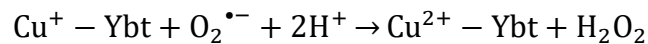
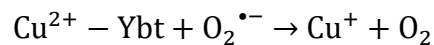


Figure 4: Incomplete reductions of molecular oxygen and main detoxification mechanism for some of the reactive species created. Numbers indicate the order of the reactions for the detoxification process to regenerate the initial redox state of the enzyme.

When the CopA/CueO system is overwhelmed, *E. coli* induces the expression of the Cu sensing (Cus) system (Figure 3), allowing periplasmic and cytoplasmic Cu to be expelled out of the cell by the CusCBA efflux pump (Bondarczuk and Piotrowska-Seget, 2013; Hobman and Crossman, 2015; Kim *et al.*, 2011; Ladomersky and Petris, 2015; Solioz, 2018).

The last system is the plasmid-born copper (Pco) resistance system (Figure 3) found in *E. coli* isolated from pigs fed with Cu-supplemented food. It uses the two-component PcoRS to induce *pcoABCDRS* and *pcoE*. Briefly, this system is believed to rely mainly on the CueO related MCO, PcoA and the efflux pump PcoB (Bondarczuk and Piotrowska-Seget, 2013; Hobman and Crossman, 2015; Ladomersky and Petris, 2015; Lawarée *et al.*, 2016; Solioz, 2018).

However, MCOs and efflux pumps are not the sole way bacteria possess to cope with Cu. *Pseudomonas aureofaciens* uses its exopolysaccharides to physically block Cu ions from reaching its cell wall (Bondarczuk and Piotrowska-Seget, 2013; González *et al.*, 2010) (Figure 3). *E. coli* siderophore, yersiniabactin (Ybt), is able to form complexes with Cu²⁺ thus preventing its reduction into the more toxic Cu⁺ and its intracellular penetration (Figure 3) (Chaturvedi *et al.*, 2012). Moreover, these Ybt-Cu²⁺ complexes seems to be able to catalyze O₂^{•-} dismutation (Chaturvedi and Henderson, 2014; Chaturvedi *et al.*, 2014).



3. Oxidative stress

Oxidative stress appeared with the rise of O₂ in the atmosphere (Solioz, 2018). They are defined as a shift in the oxidants/anti-oxidants equilibrium towards the oxidants, leading to a disruption in the redox signaling and control and/or molecular damages to either lipids, nucleic acids or proteins (Sies, 2015). This shift is often due to an abnormal exposure or production of reactive species (RS). RS can be classified by the element they originate from *i.e.* ROS for RS derived from O₂ (Figure 4), reactive nitrogen species (RNS) for those derived from nitrogen, and the same goes for a series of elements. They can also be separated between radical and non-radical species (Sies *et al.*, 2017). Two important factors of RS are their reactivity and, directly linked to that, their stability. Indeed, more stables RS like H₂O₂ tend to do fewer damages than more reactive species such as HO[•]. However, the more stable RS tend to spread more inside the cell whereas the damages generated by more reactive RS will display a shorter range of action. ROS and particularly the ones generated from incompletes reductions of O₂, *i.e.* O₂^{•-}, HO[•] and H₂O₂ are the most studied RS (Figure 4).

Among them, O₂^{•-} and H₂O₂ can be detoxified by superoxide dismutase (SOD) and catalase/peroxidase, respectively (Figure 4). Other detoxification mechanisms involving natural antioxidants like ascorbic acid or glutathione also exist (more details on some of those mechanisms in the part related to *C. crescentus*) (Gardès-Albert *et al.*, 2003).

Resistance against heavy metals like Cu and oxidative stress requires the synthesis of a lot of proteins for the sole purpose of surviving with not many others benefit. If this strategy is the sole available for weakly-motile bacteria, some of the motile ones might rely on a process called chemotaxis to detect and avoid those noxious compounds as well as having the benefit to detect favorable compounds and aim toward them.

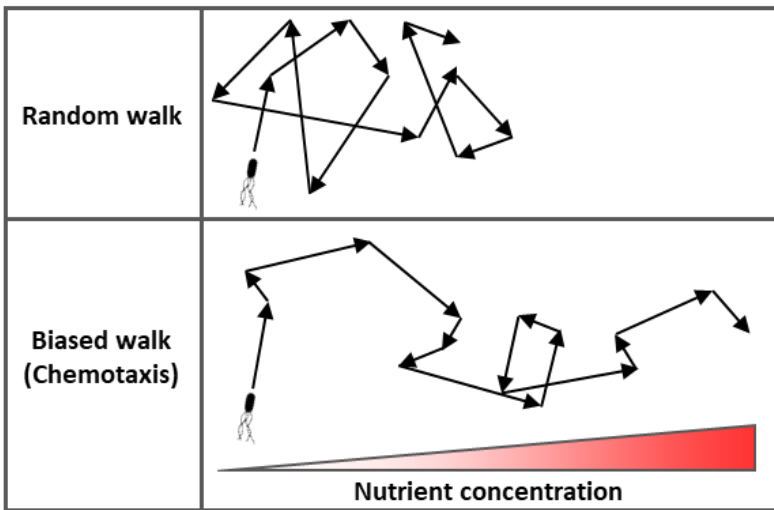


Figure 5: Random walk vs biased walk comparison. Each arrow represent a step *i.e.* a straight forward movement for a certain period of time (represented by the length of the arrow). Each step is followed by a random change of direction. Random walk: the step length is random for each step. Biased walk: the length of a step depend if the bacteria is swimming toward an increasing nutrient concentration or not.

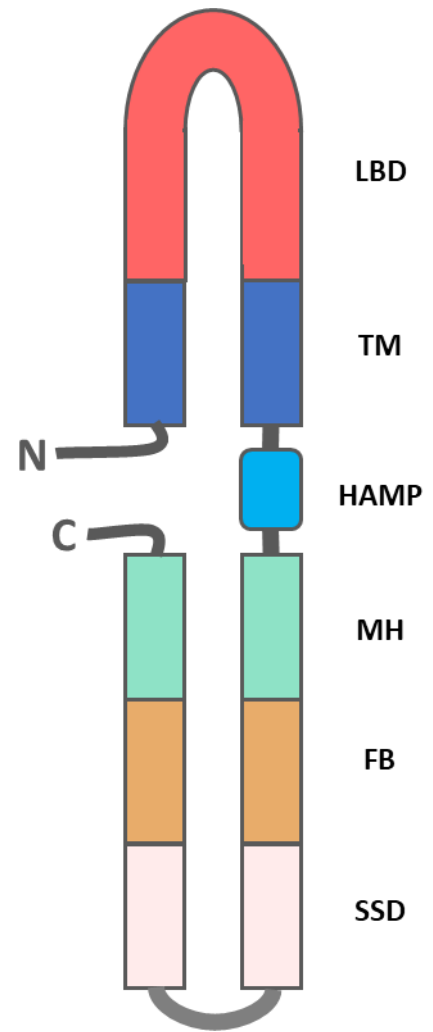


Figure 7: Structure of a methyl-accepting chemotaxis protein. LBD: ligand binding domain. TM: transmembrane helices. HAMP: Histidine kinase, Adenyl cyclase, Methyl-accepting chemotaxis proteins and Phosphatase region. MH: methyl-accepting chemotaxis proteins and Phosphatase region. FB: flexible bundle. SSD: signaling subdomain

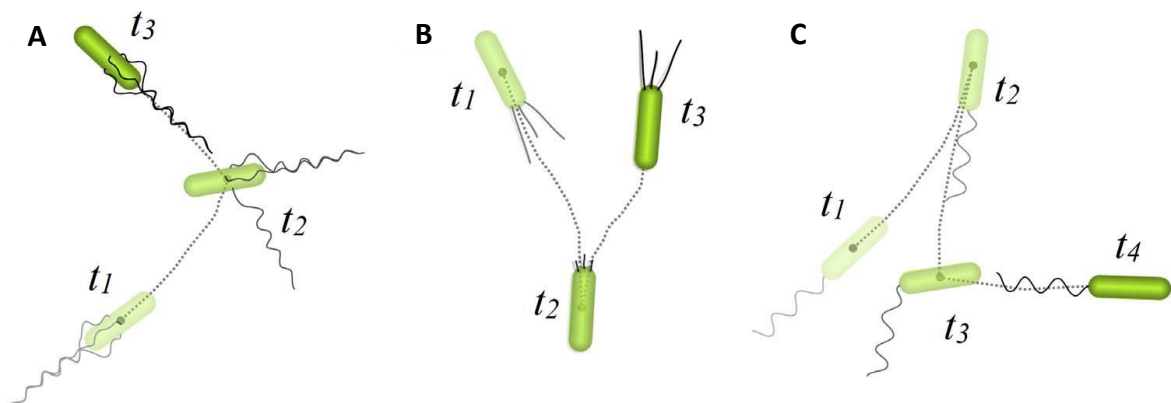


Figure 6: Motility patterns of swimming bacteria. **A.** Run-and-tumble. **B.** Forward-backward. **C.** Forward-backward-flick.

4. Chemotaxis

4.1. Movements

Every organism has its own way to sense its environment. For this purpose, many flagellated bacteria rely on a mechanism called chemotaxis. Chemotaxis is based on two movements: a straightforward swimming for a determined time (*i.e.* a step of a determined length in modelizations) and a random change of direction between each step. Chemotaxis uses a biased walk method to direct bacteria in their environment. Opposite to random walk, where the length of every step and the changes of direction are both random, biased walk step length is increased toward favorable compounds (chemoattractants) and decreased toward the noxious ones (chemorepellents) (Figure 5). Thus, the overall progress of a biased walk is far superior to a random one. As mentioned before, in both methods the changes of directions are random and happen when one or more bacterial flagella change their directions of rotation.

Different bacteria possess a different number of flagella, this led to the apparition of different motility patterns: most of the multiflagelleted bacteria move according to the “run-and-tumble” pattern whereas the uniflagelleted ones often follow either the “forward-backward-flick” or the “forward-backward” pattern (Figure 6). Possessing 4 to 6 flagella, *E. coli* follows the “run-and-tumble” pattern (Figure 6). When all flagella rotate counter-clockwise (CCW) the bacterium swims straightforward (run). This movement is only interrupted when one or several flagella change their sense of rotation to clockwise (CW), inducing a sudden change of direction of the bacteria (tumble). On another hand, some uniflagellated bacteria like *C. crescentus* follow the “forward-backward-flick” pattern (Figure 6). When the flagellum rotates CW, the bacterium swims straightforward (forward). When the flagellum changes its sense of rotation to CCW, the bacterium reverses its swim (backward) and a tension starts to accumulate at the base of the flagellum. When the flagellum changes back its direction of rotation, the accumulated tension is released, leading to a change of direction of the bacteria (flick). One last model is the simpler “forward-backward” model (Figure 6) where bacteria perform turning angles of almost 180°. This model is often found in marine bacteria (Taktikos *et al.*, 2013).

4.2. Signal sensing

Chemoattractants and chemorepellents are sensed by chemoreceptors called methyl-accepting chemotaxis proteins (MCPs). MCPs are often localized in the cytoplasmic membrane but some of them are cytosolic. MCP structure is composed of a ligand binding domain (LBD), able to bind ligands directly or through binding proteins; transmembrane helices (TMH); and a cytoplasmic signaling domain (SD) (Figure 7). The SD is subdivided into a Histidine kinase, Adenyl cyclase, Methyl-accepting chemotaxis proteins, and Phosphatase (HAMP) region, responsible to transfer the signal from the LBD to the rest of the SD; methylation helices (MHs), where glutamate residues can be methylated/demethylated by the couple methyltransferase/methylesterase CheR/CheB responsible for the adaptive system; a flexible bundle (FB) where a conserved glycine hinge is important for the formation of supramolecular MCPs complexes; and a signaling subdomain (SD) that interacts with the adaptor protein CheW and the histidine kinase CheA to transfer the sensed signal to the flagellar motor (Salah Ud-Din and Roujeinikova, 2017; Wadhams and Armitage, 2004). An analysis over 3524 MCPs sequences classified them into 7 different topologies (Ia, Ib, II, III_m, III_c, IV_a, and IV_b) based

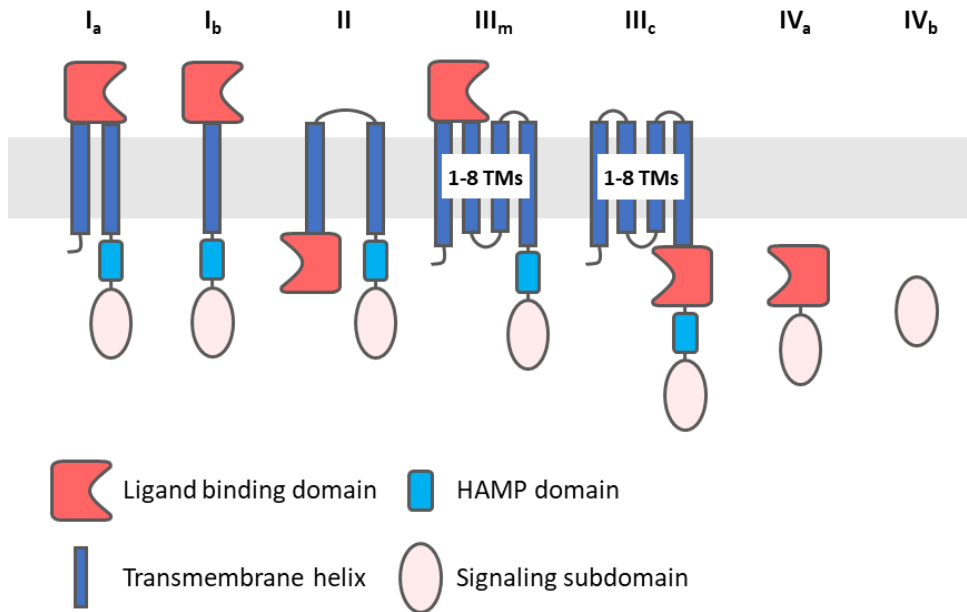


Figure 8: Local classification of methyl-accepting chemotaxis protein based on their topology.

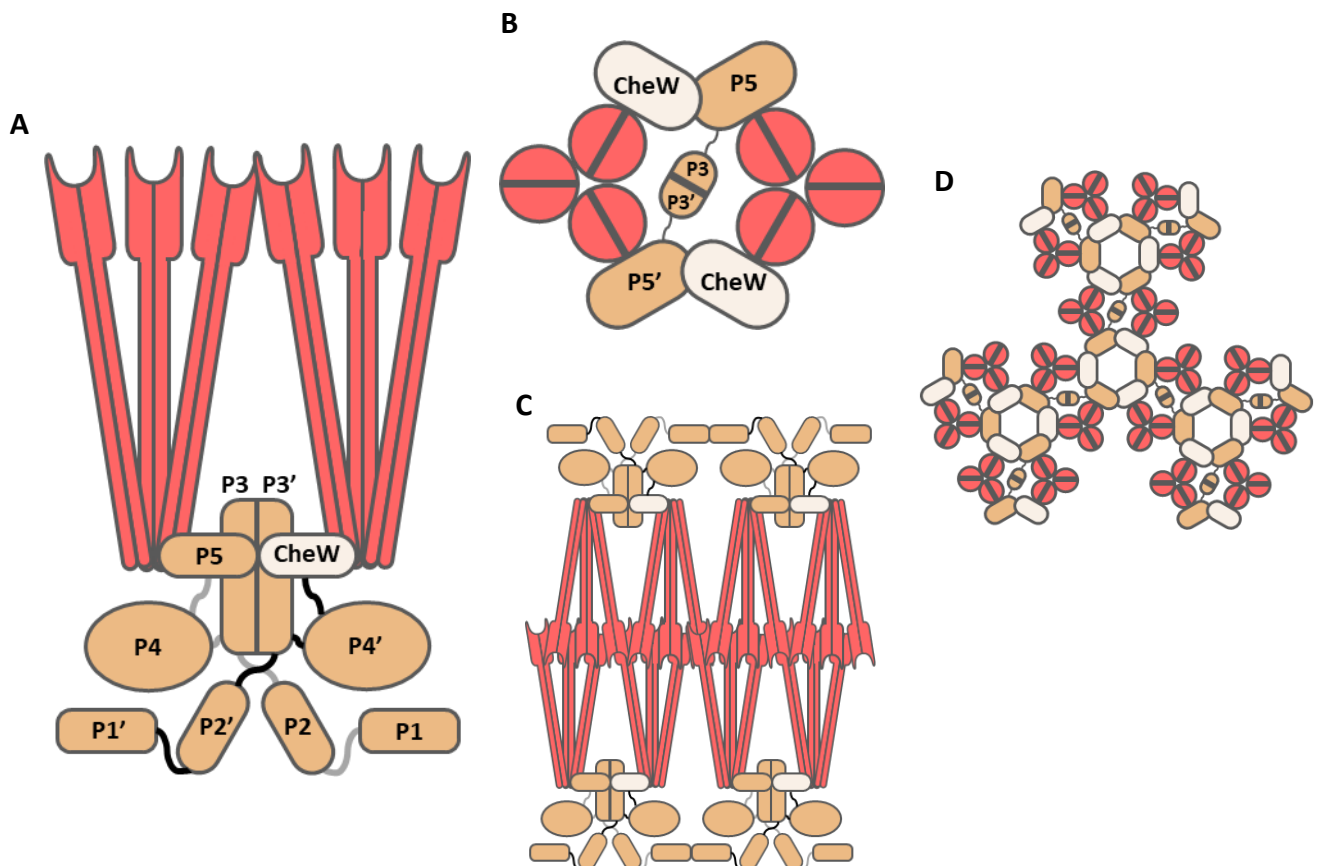


Figure 9: Supramolecular structures of MCP in association with CheA and CheW. **A.** Core complex. **B.** Core complex 90° rotation. **C.** Sandwich-like structure of cytoplasmic MCPs core complexes. **D.** Sensing array pattern.

on the number of TMHs and the presence and the position of the LBD (Figure 8) (Lacal *et al.*, 2010; Salah Ud-Din and Roujeinikova, 2017).

Membrane-bound MCPs assemble into dimers then into trimers of dimers along with two CheA and two CheW to form the core complex (Figure 9A, B), *i.e.* the minimal unit capable of sensing and transmitting the signal. Cytoplasmic MCPs assemble into sandwich-like structures composed of 2 CheA-CheW plates with the 2 MCPs arrays at the center with LBDs facing each other (Figure 9C). Those core complexes pack hexagonally to form sensing arrays that can contain thousands of proteins (Figure 9D) (Collins *et al.*, 2014; Parkinson *et al.*, 2015; Salah Ud-Din and Roujeinikova, 2017). Membrane-bound MCPs sensing arrays tend to have polar localizations inside the cell although some exceptions exist. Cytoplasmic MCPs arrays are either polar or dispersed along the cell body (Salah Ud-Din and Roujeinikova, 2017). As an example for these localizations, *Rhodobacter sphaeroides* possess mainly polar clusters and minor smaller lateral clusters, as well as a mid-cell cytoplasmic cluster (Jones and Armitage, 2015).

4.3. Signal transduction

E. coli chemotaxis uses the following mechanism (Figure 10). In absence of chemoattractants or upon chemorepellents binding by the cognate MCP, the signal will induce a trans-autophosphorylation of the histidine kinase CheA. Then the phosphate group will be transferred to an aspartate residue of the response regulator CheY. CheY~P freely diffuse through the cytoplasm and is able to interact with two proteins of the flagellar motor switch complex by binding to the C-terminal region of FliM and interacting with FliN to induce a change in the rotation direction of the flagellum (CCW to CW) (Sarkar *et al.*, 2010). The signal is then terminated by the action of the constitutively active phosphatase CheZ on CheY~P letting the flagellum switch back to a CCW rotation. However, upon chemoattractant binding by the cognate MCP, CheA remains unphosphorylated and inactive thus letting the flagella rotate in CCW direction. This defines a basic kinase ON/OFF mechanism that is supported by an adaptative branch allowing the bacterium to know whether the concentration of chemoattractant/repellent is increasing or decreasing (Hazelbauer *et al.*, 2008; Wadhams and Armitage, 2004).

4.4. Adaptative system

When moving along a gradient, it is important for bacteria to determine the position of the source of the gradient. So, bacteria compare the current concentration sensed to the previous one using the adaptive system. Typical MCP adaptation in *E. coli* occurs by methylation and demethylation of the MHs glutamates residues. On one hand, the methyltransferase, CheR, is able to methylate glutamate residues in the MHs of MCPs thus increasing their ability to phosphorylate CheA. On the other hand, in addition to CheY, CheA is able to phosphorylate the methylesterase CheB. CheB~P is then able to demethylate MHs, thus decreasing the ability of the MCP to activate CheA. This adaptation will have the following effect: when bacteria are stuck in an environment where the concentration of chemoattractants remains unchanged, the MCPs will tend to phosphorylate CheA thus increasing the number of direction changes of bacteria (Collins *et al.*, 2014; Wadhams and Armitage, 2004).

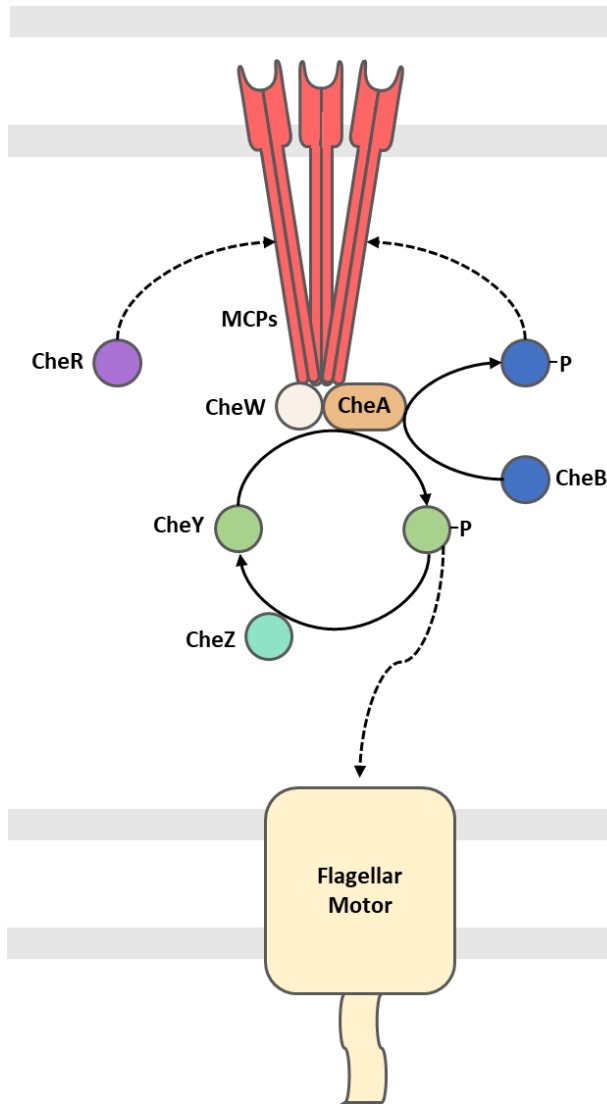


Figure 10: Signal sensing and transduction and adaptation by a classical bacterial chemotaxis system.

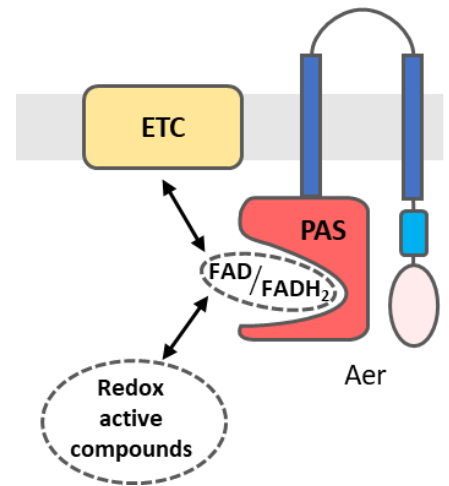


Figure 11: Model of aerotaxis and energy taxis by *Escherichia coli* chemoreceptor Aer.

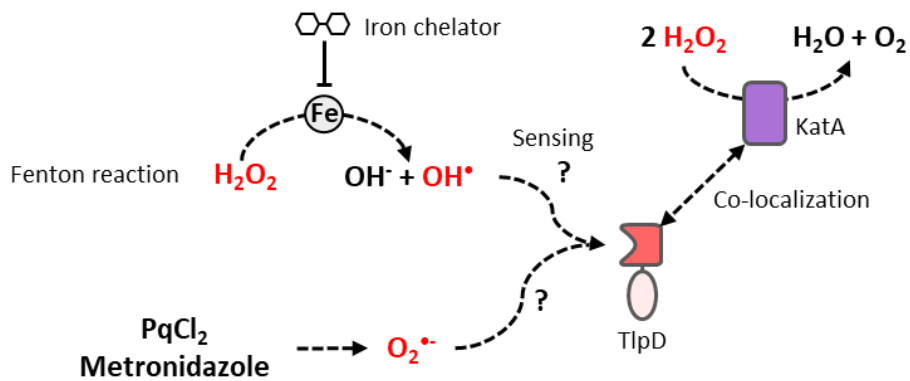


Figure 12: Model of ROS sensing by *Helicobacter pylori* chemoreceptor TlpD.

4.5. Sensory repertoire

4.5.1. *Escherichia coli* Aer

E. coli Aer is a membrane-anchored cytoplasmic MCP and is believed to be an aerotaxis/energy taxis receptor (Figure 11). Aer works by sensing the redox state change of a flavin adenine dinucleotide (FAD) molecule bound to its sensory PAS domain by a conserved tryptophan residue. FAD redox changes within the PAS domain are likely to occur by interaction with the electron transport chain or cytoplasmic redox-active compounds (Alexandre, 2010). Those redox changes will induce or not the MCP transphosphorylation.

4.5.2. *Helicobacter pylori* TlpD

H. pylori is a Gram-negative bacterium known to colonize human stomach. As stomach is a harsh environment with a very acidic pH in the lumen (pH 5 to 1), *H. pylori* needs to find a suitable environment: within 15 μm from gastric epithelial cells and deep within gastric glands. The colonization of these environments is partly driven by chemotaxis. To this purpose, *H. pylori* possess 3 transmembrane MCPs (TlpA, TlpB, and TlpC) and a cytoplasmic polar-localized one (TlpD) (Johnson and Ottemann, 2018). TlpD has recently been found to sense cytoplasmic OH^\bullet generated by the Fenton reaction as well as $\text{O}_2^\bullet^-$ (Figure 12). A strain lacking all MCPs except TlpD was found to react to both Fe and H_2O_2 . However, preincubation of the strain with a membrane permeable Fe chelator seemed to inhibit the response to H_2O_2 . This led the hypothesis that TlpD was sensing ROS generated by the Fenton reaction instead of Fe and H_2O_2 directly. TlpD was also able to sense paraquat dichloride and metronidazole, two compounds known to generate ROS (Collins *et al.*, 2016). Furthermore, TlpD seems to colocalize with the catalase KatA at the cellular poles, thus reinforcing its link with oxidative stress (Behrens *et al.*, 2016).

5. *Caulobacter crescentus*

C. crescentus is a free-living α -proteobacteria mostly found in oligotrophic aqueous environments. It is used as a model to study the cell cycle and the differentiation due to its dimorphic nature. Indeed, upon cell division, *C. crescentus* generates 2 distinct morphotypes: 1) a motile form with a polar flagellum and two pili, called the swarmer cell (SW) and 2) a sessile, substrate-bound form by a stalk, the stalked cell (ST).

5.1. Redox state & Cell cycle

The SW cell swims in its environment until it finds an appropriate niche (Figure 13). It will then begin its differentiation into a ST cell by losing its flagellum, retracting its pili and synthesizing a stalk at the same pole. The tip of this stalk is covered by a polysaccharidic holdfast, allowing the ST cell to stick to a substrate. DNA replication will occur in the ST cell with the elongation up to a predivisional (PD) cell that will synthesize a new flagellum at opposing pole of the stalk. This PD cell will then divide asymmetrically into a ST cell and a new SW cell (Curtis and Brun, 2010).

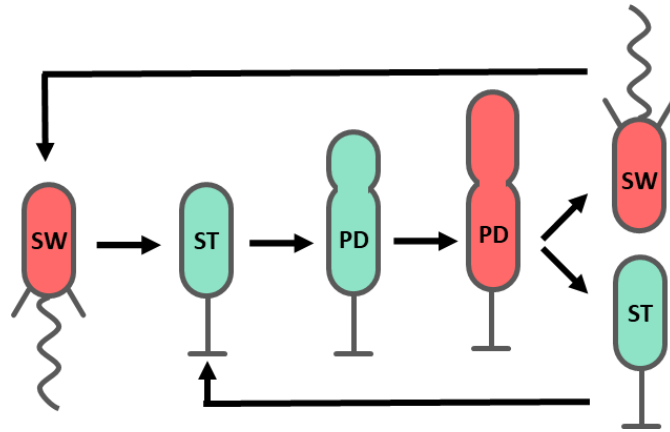


Figure 13: *C. crescentus* model of cell cycle and asymmetric division. Colors represent the cytoplasmic redox state of the cell type. Green: more oxidizing. Red: more reducing. SW: swarmer cell. ST: stalked cell. PD: predivisional cell.

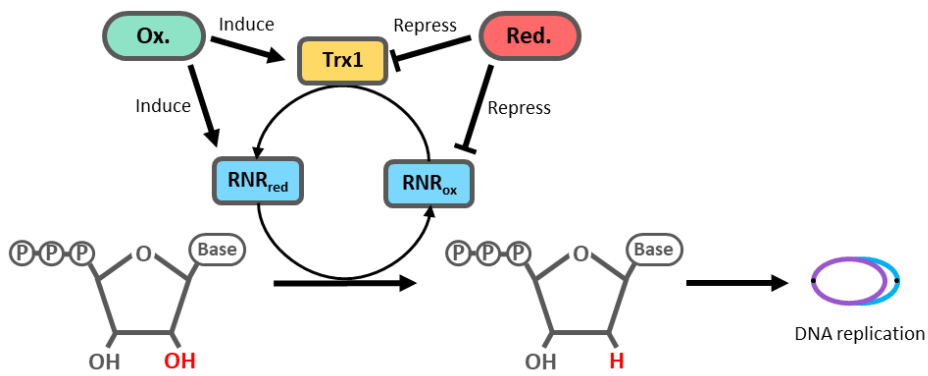


Figure 14: Influence of *C. crescentus* cytoplasmic redox state on DNA replication. Colors represent the cytoplasmic redox state of the cell type. Green: more oxidizing. Red: more reducing. RNR: ribonucleotide reductase. Trx: Thioredoxine

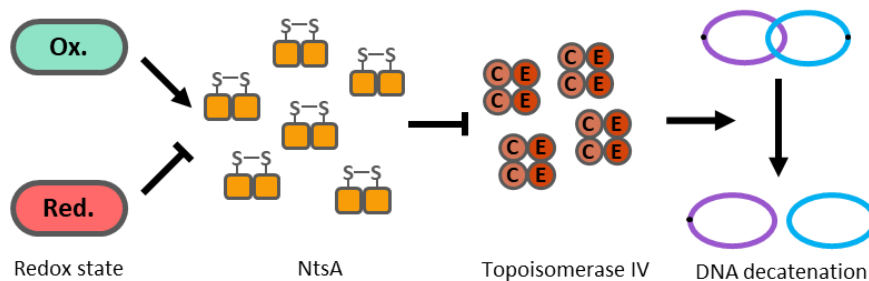


Figure 15: Influence of *C. crescentus* cytoplasmic redox state on DNA decatenation. Colors represent the cytoplasmic redox state of the cell type. Green: more oxidizing. Red: more reducing.

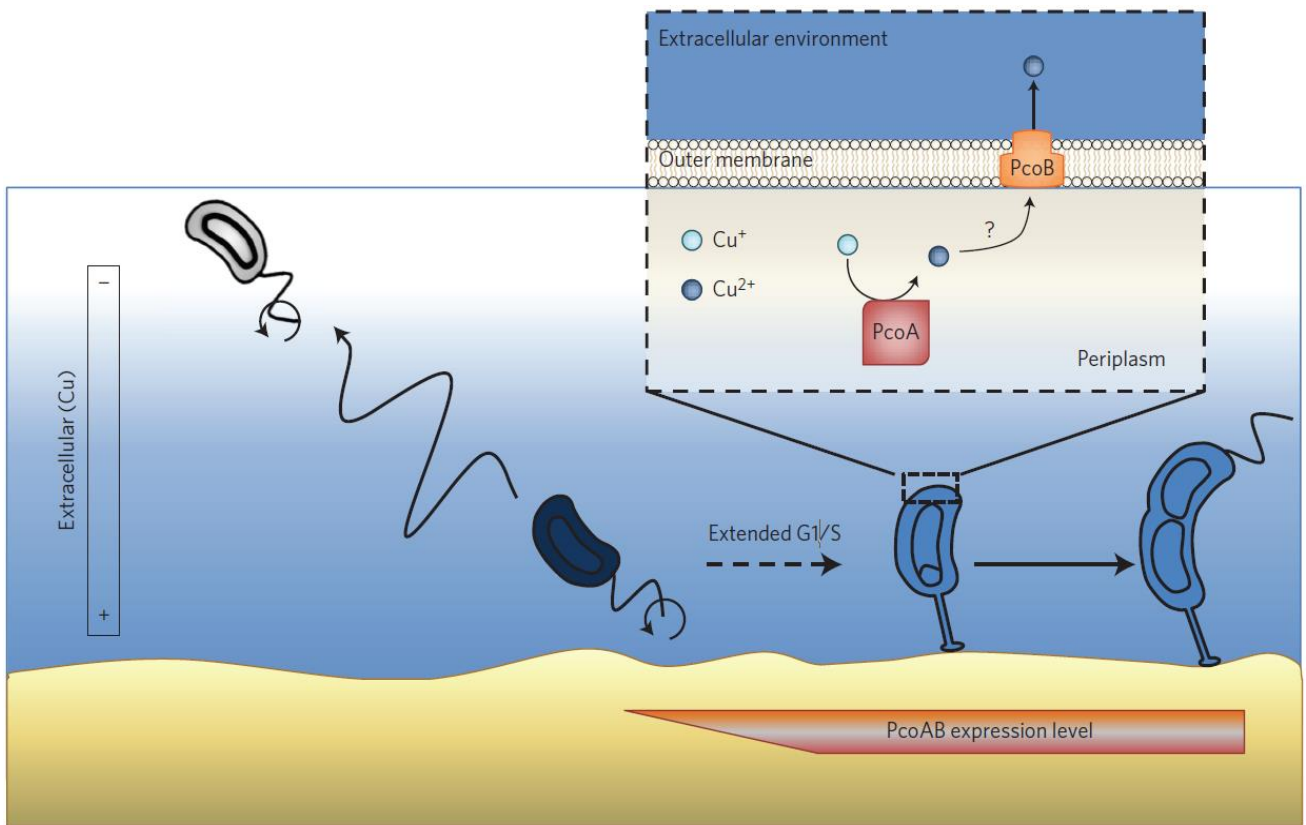


Figure 16: Model of the *C. crescentus* bimodal response. In a Cu-rich environment, the ST cell triggers a Cu detoxification relying on the cell type-specific PcoAB defense system. In the same context, the SW cell accumulates a high level of Cu, which may act as an internal cue to escape towards a Cu-free environment.

C. crescentus cellular redox state varies along the cell cycle. SW cells cytoplasm is in more reducing state and becomes more oxidizing when differentiating into ST cells and PD cells. PD cells will then switch back to a reducing state prior to cell division (Figure 13) (Narayanan *et al.*, 2015). This redox switch is very important to at many steps of the cell cycle.

It is needed for a correct DNA replication. Indeed, it has been shown that *C. crescentus* ribonucleotide reductase (RNR) is expressed in the early stage of PD cells when the cytoplasm is in a more oxidizing state (Figure 14). However, after catalyzing the reduction of a ribonucleotide into the corresponding deoxyribonucleotide, the RNR needs to be reduced in order to catalyze further reactions. This is thought to be the role of the unique thioredoxin (Trx) of *C. crescentus*, Trx1. Trxs catalyze the reduction of oxidized cysteine (Cys) residues and thus are involved in oxidative stress defenses as well as in a couple of signal transduction pathways. Trx1 is expressed together with RNR during the early stage of PD cells and proteins with similar folds were already been shown to reduce RNR. This led to the suggestion that Trx1 is responsible for the reduction of RNR thus allowing the synthesis of the deoxyribonucleotides required for DNA replication (Goemans *et al.*, 2018).

Moreover, the redox switch seems also important to avoid early chromosome decatenation (Figure 15). Indeed, the topoisomerase IV complex, involved in the chromosome decatenation, is inhibited by active NtsA. NstA activation is required for the formation of intramolecular disulfide bonds. So, when the cytosol is in the more oxidizing state, *i.e.* in early PD state when the DNA is replicating, NstA can form dimers by forming disulfide bonds, and thus is able to bind the ParC proteins of the topoisomerase IV complex, inhibiting its activity. When DNA replication is over and the cytoplasm is back in a more reducing state, the topoisomerase IV is then active and able to decatenate the chromosomes (Narayanan *et al.*, 2015).

5.2. Response to Cu stress

Although the Cue and Cus systems are conserved, they do not seem to be part of the main response of *C. crescentus* against Cu stress. *C. crescentus* rather exhibits a unique response for a bacterium (Figure 16). It presents a bimodal response to Cu stress. Indeed, STs use a genetically-encoded and cell cycle-regulated PcoAB system, whereas SWs flight from Cu source. Inside the ST cells, cytoplasmic PcoA detoxifies Cu⁺ into Cu²⁺. Cu²⁺ is then expelled from the cytoplasm by PcoB. The SW cells accumulate Cu and then trigger a flight response within a minute to find a Cu-free environment. This flight response is thought to be mediated by a chemotaxis system (Lawaarée *et al.*, 2016).

5.2.1. Chemotaxis

As mentioned previously, *C. crescentus* SW is a uniflagellated bacterium swimming according to the “forward-backward-flick” pattern. *C. crescentus* chemotaxis is not very well understood. Even if most of the proteins related to chemotaxis seems conserved in *C. crescentus*, some genes found in two chemotaxis operons of *C. crescentus* (*cheD*, *cheL*, *cheU*, *cheE*, and *cheX*) have currently unknown functions. *C. crescentus* have 19 MCPs present in either one of the two chemotaxis operons or split around the rest of its genome. Among those 19 MCPs, 12 are predicted transmembrane MCP among which 2 of them possess a predicted cytoplasmic LBD. The 7 last MCPs are predicted to be cytoplasmic. Furthermore, *C. crescentus* have 2 predicted CheA homologs, 4 CheW, 3 CheR, 2 CheB, and 12 CheY but lack a copy of CheZ. Some of

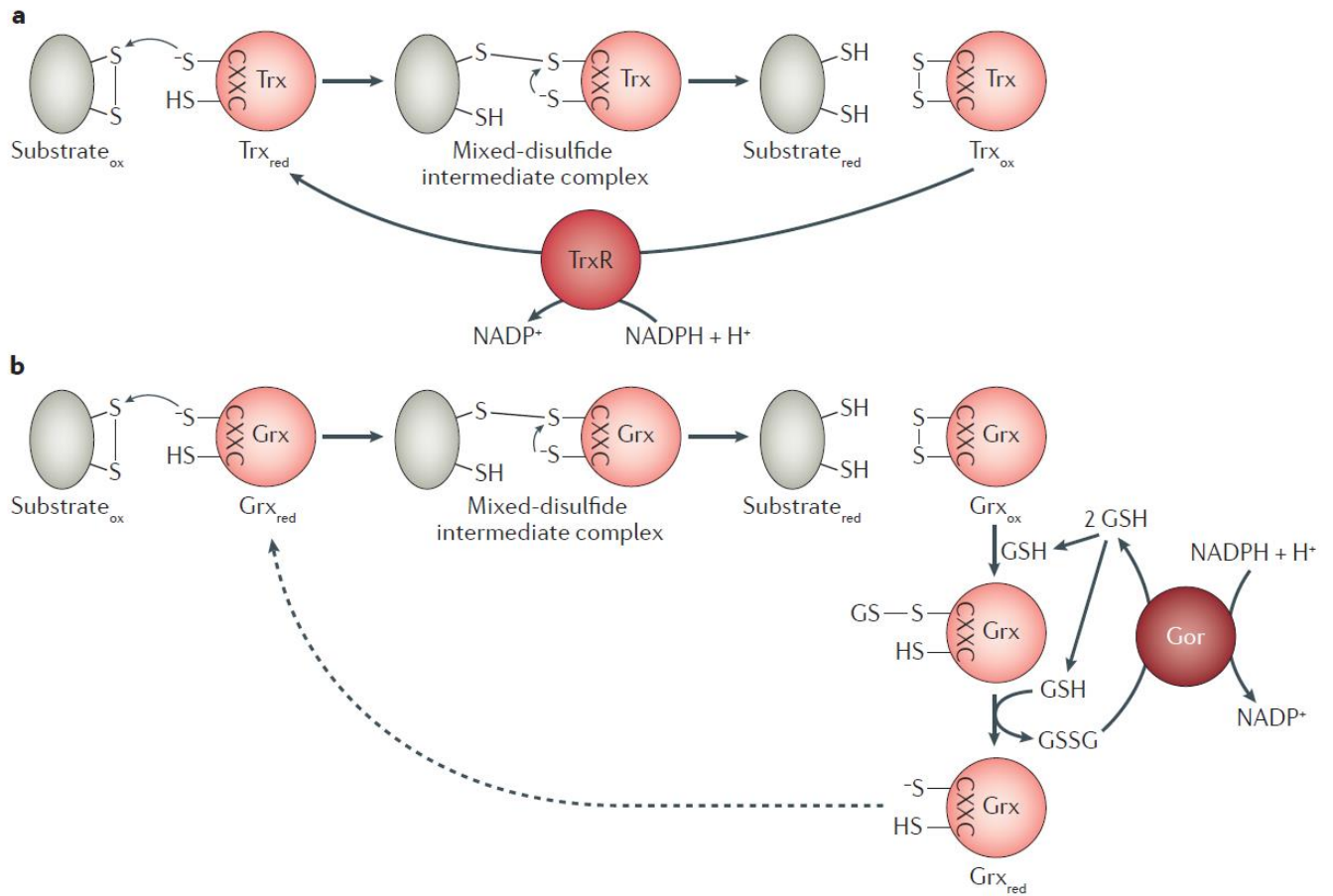


Figure 17: Mechanisms of Trx and Grx activity. **A.** Reduction of a disulfide bond in a substrate protein by a Trx. **B.** Reduction of a disulfide bond in a substrate protein by a Grx

the CheY homologs have recently been described as involved in attachment of *C. crescentus* to the substrate when the flagellum hits the latter and have been renamed Cle, standing for CheY-like cyclic-di-GMP effectors (Nesper *et al.*, 2017). The functions of the others CheY homologs have not been tested so far but the main hypothesis is that some of them may act as a phosphate sink. This hypothesis is supported by the fact that some closely related bacteria like *Sinorhizobium meliloti* use the same mechanism to counteract the absence of CheZ (Amin *et al.*, 2014). *C. crescentus* seems to possess proteins with unknown function that are probably involved in chemotaxis due to their presence in chemotaxis operons. Those are CheD, CheE, CheL, and CheU. Homologs of CheD are found in other bacteria but the other 3 seem specific to *C. crescentus*.

5.3. Defenses against oxidative stress

5.3.1. Thioredoxins, glutaredoxins & glutathione

Trxs are involved in the reduction of oxidized Cys residues (Figure 17). They are involved in regular metabolism as explained earlier with the reduction of the RNR to keep its metabolic activity active. However, Trxs are also involved in the reduction of non-native oxidized Cys residues that can arise upon oxidative stress. The N-terminal Cys of the conserved catalytic motif is present as a thiolate under physiological conditions. This thiolate will attack an oxidized Cys residue to form a mixed-disulfide intermediate. This will trigger the deprotonation of the second Cys residue. This deprotonated Cys then attacks the mixed disulfide intermediate releasing an oxidized Trx and a reduced target protein. The Trx will then be regenerated by the Trx reductase (Ezraty *et al.*, 2017). As explained previously, *C. crescentus* expresses only one cell cycle-regulated Trx, Trx1 (Goemans *et al.*, 2018).

Glutaredoxins (Grxs) are enzymes related to Trx, possessing either a CXXC or a CXXS catalytic motif. Grxs with a CXXC motif reduce oxidized Cys in a similar way as Trx proteins but are reduced by the low-molecular-weight thiol glutathione (GSH) (Figure 17). GSH reacts with the N-terminal Cys to form a mixed-disulfide intermediate that reacts with a second GSH molecule, releasing a reduced Grx and an oxidized glutathione molecule (GSSG). GSH can also act alone as a redox buffer by reacting with the RS as well as reacting with sulfenic acids to prevent the irreversible oxidation of Cys residues into sulfenic and sulfonic acids (Ezraty *et al.*, 2017). *C. crescentus* genome is predicted to encode 3 Grxs.

Some *C. crescentus* genes related to these proteins were found to be upregulated under cadmium stress (Hu *et al.*, 2005)

5.3.2. Catalase-peroxidase – KatG

Catalases-peroxidases are enzymes with multiple activities. Although the main activity is the catalase with a $k_{\text{cat}} \sim 5000 \text{ s}^{-1}$, close to what is observed in monofunctional catalases. The next predominant activity is the peroxidase with a $k_{\text{cat}} \sim 50 \text{ s}^{-1}$. The other activities are marginal with k_{cat} less than 1 s^{-1} . Catalase and peroxidase activities both possess a common first part with a two electrons reduction of H_2O_2 into H_2O (Figure 18) but differ on the oxidative part used as a catalytic turnover. On one hand, the catalase turnover involves a two electrons oxidation of a second H_2O_2 molecule into O_2 . On the other hand, the peroxidase turnover involves one-electron oxidations that can happen on a wide variety of aromatic compounds, turning them

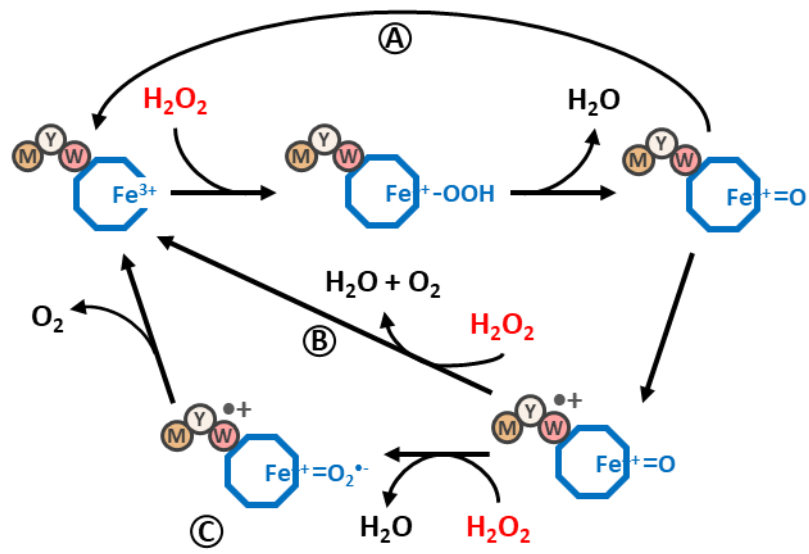


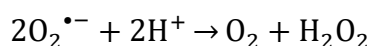
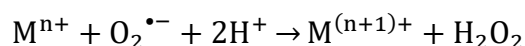
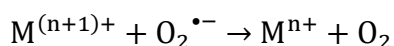
Figure 18: Working model of the catalase peroxidase KatG

into their corresponding radicals. Surprisingly, the active site of *katG* is closer to a peroxidase catalytic site than a catalase one but, as mentioned earlier, this is the predominant activity of *katG*. This fact is explained by the involvement of two cofactors: a heme b, a rather common cofactor; and a methionine-tyrosine-tryptophan (MYW) adduct, a tri amino acid moiety with a post-transcriptional link of their lateral chains. This cofactor seems to be unique to *katG*. The first of the catalytic activity of *katG* is the reduction of an H₂O₂ molecule. The H₂O₂ will react with the Fe³⁺ ion of the heme b cofactor to form the ferryl porphyrin cationic radical π (Fe⁴⁺=O[por]^{•+}) by releasing an H₂O molecule. Then the turnover will differ depending on the activity. Three mechanisms are currently proposed for the catalase activity: 1) a direct conversion of Fe⁴⁺=O[por]^{•+} into the initial Fe³⁺ state (Figure 18A) 2) the formation of the Fe⁴⁺=O[MYW]^{•+} intermediate followed by a return to the initial Fe³⁺ state (Figure 18B) or 3) the formation of the Fe⁴⁺=O[MYW]^{•+} intermediate with then the formation of the Fe³⁺—O₂^{•-} [MYW]^{•+} intermediate before a come-back to the initial Fe³⁺ state (Figure 18C). The peroxidase turnover only has one proposed mechanism involving both a tryptophan and a tyrosine residue as electrons sources for the reduction of the Fe⁴⁺=O[por]^{•+} (Njuma *et al.*, 2014).

Little is known about *C. crescentus katG*. It seems to be part of the OxyR regulon, the main transcriptional factor activated in H₂O₂ stress and is also induced in the stationary phase. *KatG* seems to be localized in both cytoplasmic and periplasmic spaces (Italiani *et al.*, 2011; Schnell and Steinman, 1995; Steinman *et al.*, 1997).

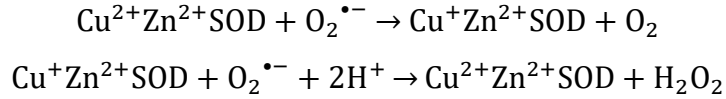
5.3.3. Superoxide dismutases – SodA, SodB & SodC

Superoxide dismutases are enzymes involved in O₂^{•-} detoxification into H₂O₂ and O₂. This reaction occurs by a “ping-pong” mechanism where a reduction followed by an oxidation of a metal center will allow the oxidation of one O₂^{•-} into O₂ and the reduction of another O₂^{•-} into H₂O₂ (Abreu and Cabelli, 2010).

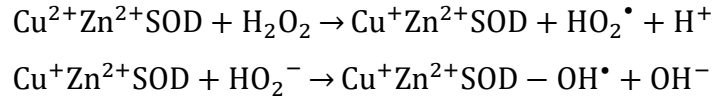


We currently distinguish 4 main categories of SODs based on their folding and their metallic cofactors: The Cu-Zn SOD, the Fe SOD, the manganese SOD and the more recently discovered Nickel SOD. Among those ones, *C. crescentus* possess two cytoplasmic SOD, a MnSOD (SodA) and a FeSOD (SodB); and a periplasmic CuZnSOD (SodC) (Abreu and Cabelli, 2010).

In bacteria, the CuZnSOD are usually either periplasmic or extracellular. This fact might not be surprising given the facts that Cu and Zn are the most stable metals in the Irving-William series and that periplasmic and extracellular spaces are environments where metalloproteins are most likely to encounter other metals. So, it is likely that the SODs found in those spaces are CuZnSOD rather than FeSOD and MnSOD, the latter probably being more sensitive to mismetallation events. They are dimeric enzymes with a catalytic site in each of the two subunits. In these subunits, the redox active metal involved in the dismutation reaction is the Cu whereas Zn plays a role in the overall enzyme stability and ensure a mostly pH-independent activity (Abreu and Cabelli, 2010).

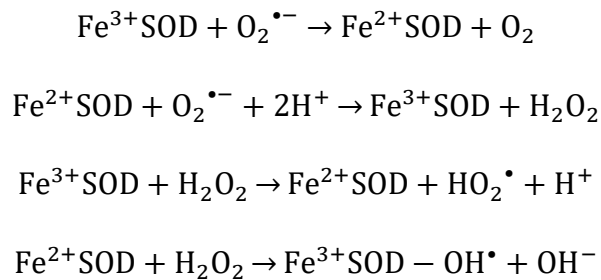


CuZnSODs are also known to possess a second catalytic peroxidase-like activity that mostly concerns the H₂O₂ generated by the dismutation. This reaction is a Fenton-like reaction where an H₂O₂ molecule generates OH[•] and OH⁻. It has been shown that the OH[•] generated at the active site might react with the histidine residues linking the Cu, leading to a loss of the Cu from the active site (Abreu and Cabelli, 2010).



C. crescentus SodC has been described as a periplasmic SOD. The presence of a periplasmic SOD in pathogenic bacteria like *B. abortus* can be easily understood as a mean of protection against the host oxidative defenses. However, in a free-living bacterium like *C. crescentus*, the presence of environmental O₂^{•-} and thus the need of a periplasmic SOD is less clear. Some authors thought that the presence of cyanobacteria in the close environment of *C. crescentus* might induce a local O₂ concentration peak during the day. This high local O₂ concentration might react with some phenolic compounds to generate O₂^{•-} (Schnell and Steinman, 1995; Steinman, 1993).

FeSOD and MnSOD both possess closely related structures that might witness a putative coevolution. Despite this putative coevolution, the metal specificity of both enzymes is widely conserved. Indeed, a mismetallation of Fe in a MnSOD leads to a huge decrease in the activity. Similar effects are observed for Mn in a FeSOD. They also differ by the number of subunits they can associate: MnSOD exists in both dimeric and tetrameric forms whereas FeSOD only appears to be dimeric. The mechanism of FeSOD is similar to the one of the CuZnSOD. Moreover, they also possess a Fenton-like peroxidative activity (Abreu and Cabelli, 2010).



The expression levels of *C. crescentus* SODs were previously tested in response to a series of heavy metals. *sodA* seems to have increased expressions level to every heavy metal tested whereas *sodB* expression level only presents a 2-fold increase when *C. crescentus* is exposed to Cd. It was proposed that SodB could act as a back-up when SodA is unable to counteract the oxidative stress alone. *sodC* expression levels never exceeded twice the basal levels under heavy metals exposure (Hu *et al.*, 2005). A hypothesis would be that either the basal expression level of *sodC* is enough to counteract a periplasmic oxidative stress generated by heavy metals or that the oxidative stress generated by the heavy metals tested was only relevant in the cytoplasm.

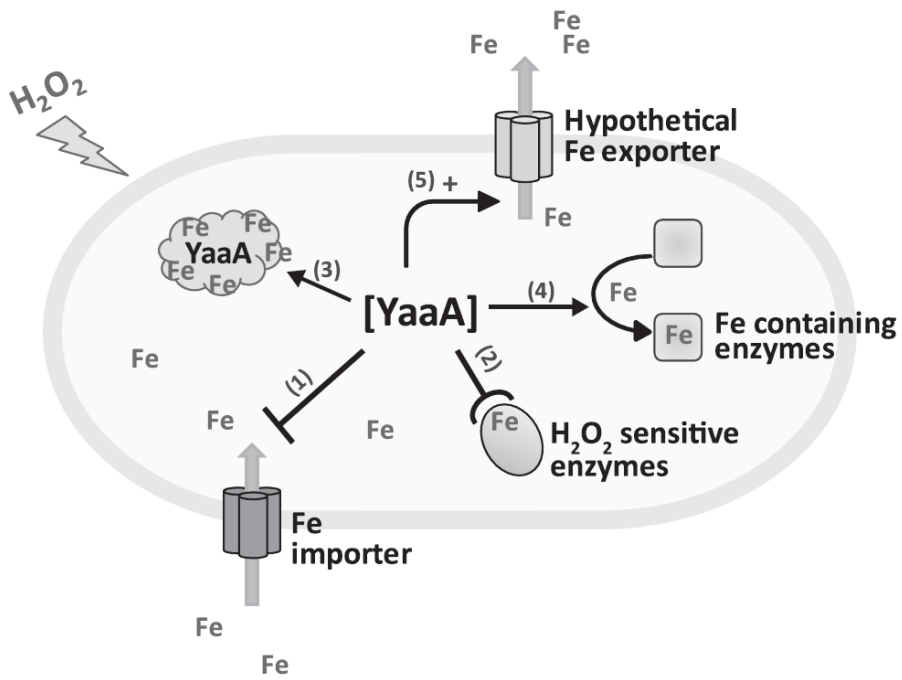


Figure 19: Putative functions of YaaA in *E. coli*

5.3.4. YaaA

In *E. coli*, YaaA is part of the OxyR regulon but only seems to be induced upon important H₂O₂ stress (Liu *et al.*, 2011) or under heavy metal cocktail exposure (Gómez-Sagasti *et al.*, 2014). It is suggested that YaaA protects the bacteria by reducing the level of free Fe thus inhibiting potential Fenton reaction that would produce important levels of OH (Figure 19). However, the mechanism by which YaaA reduces the free Fe level likely through a decrease in Fe import, an increase in Fe export, a protection against the Fe loss in enzymes hit by H₂O₂, a Fe sequestration or an increase in Fe transfer to targeted metalloproteins (Liu *et al.*, 2011).

With the already described bimodal response of *C. crescentus* to Cu (Lawarée *et al.*, 2016), one could imagine a similar response to ROS. SodABC, KatG, and Trx1 could act the main defense for the STs meanwhile the SWs would fly away from the ROS source using chemotaxis (Goemans *et al.*, 2018).

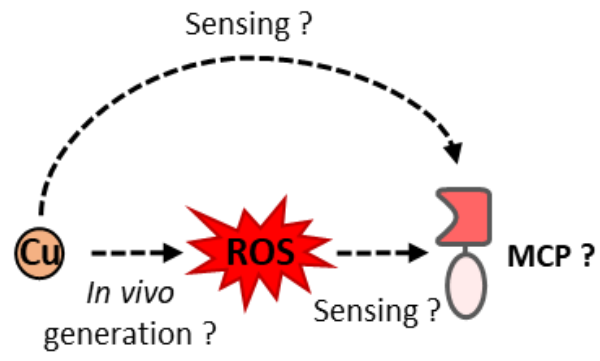


Figure 20: Model of the main hypothesis driving the master thesis.

OBJECTIVES

As described previously, upon Cu stress, *C. crescentus* engage a bimodal response. It was proposed that the SW flight is mediated by a chemotaxis pathway. In the context of Gwennaëlle Louis' thesis, several chemoreceptors were identified as putative candidates for Cu sensing. As Cu is known to generate ROS *in vitro* by a Fenton-like reaction it was hypothesized that Cu sensing could be mediated by those ROS (Figure 20). However, the pertinence of those Cu induced ROS are controversial *in vivo*. In this context, two mains questions are addressed in this master thesis: 1) Is Cu somehow able to impact the redox state of *C. crescentus*? 2) is *C. crescentus* able to fly away from oxidative stress sources?

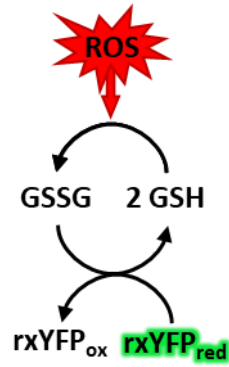


Figure 21: Working model of the redox sensitive YFP (rxYFP). ROS induce the formation of oxidized glutathione dimers (GSSG) from two reduced glutathione monomers (GSH). GSSG and GSH form an equilibrium with the oxidized and reduced rxYFP.

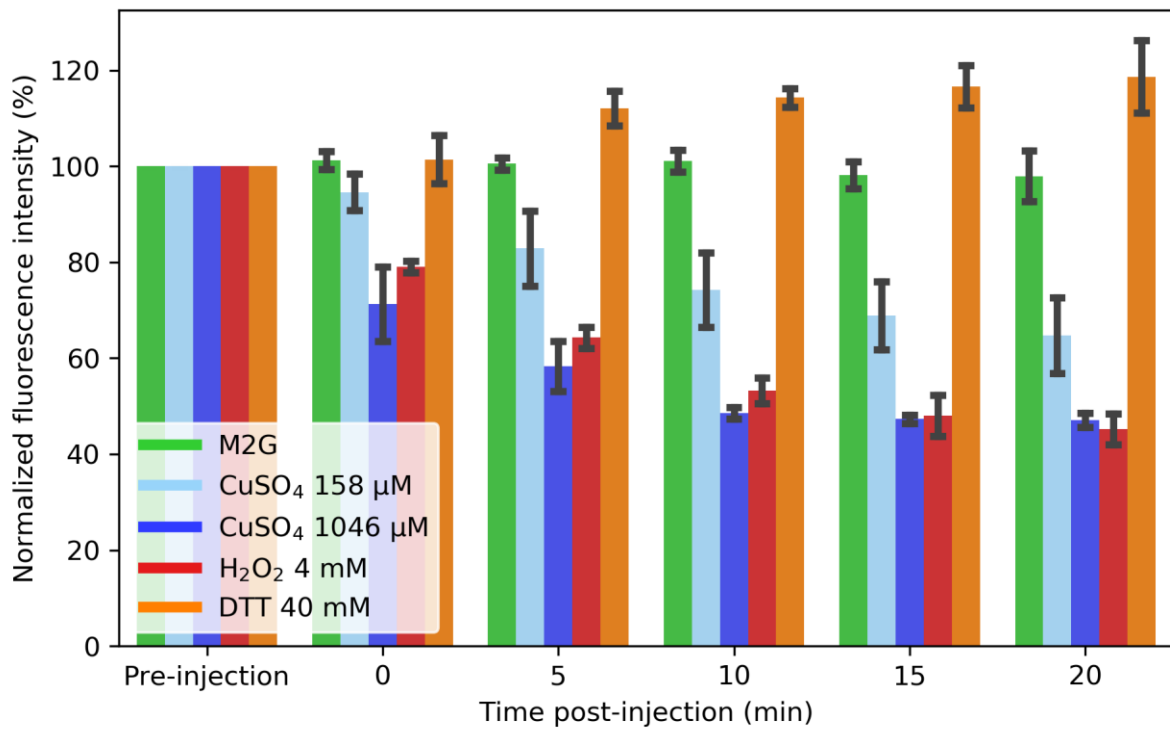


Figure 22: Over time fluorometric quantification of the cytoplasmic redox state of CB15N-rxYFP in culture medium (M2G), 158 or 1046 μM copper sulfate (CuSO₄), 4 mM hydrogen peroxide (H₂O₂) or 40 mM dithioerythiol (DTT) ($\gamma_{\text{ex}} = 509 \text{ nm}$; $\gamma_{\text{em}} = 545 \text{ nm}$) (biological replicates = 3; technical replicates = 3)

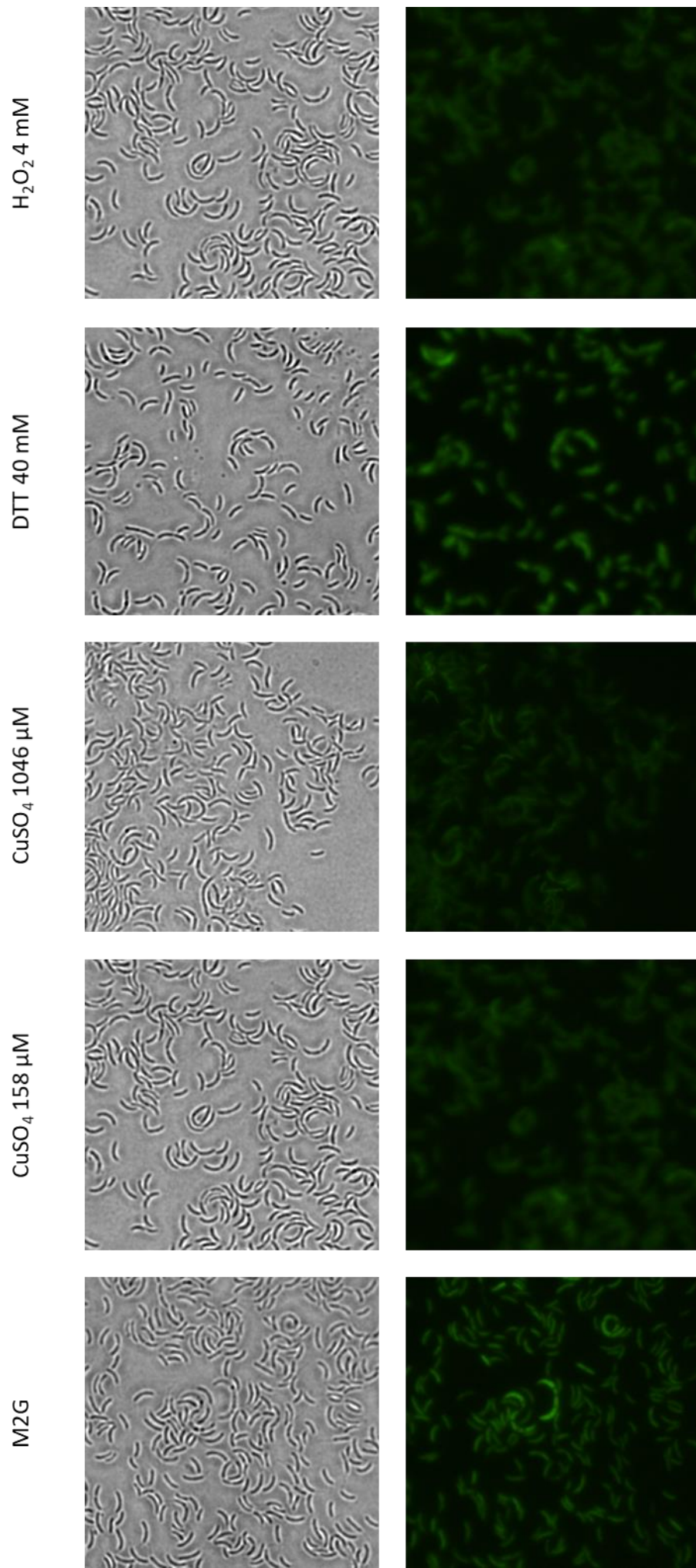


Figure 23: Microscopy pictures of CB 15N-rxYFP in culture medium (M2G) 158 and 1046 μM copper sulfate (CuSO₄), 4 mM hydrogen peroxide (H₂O₂) or 40 mM Dithioerythiol (DTT) ($\gamma_{\text{ex}} = 512 \text{ nm}$)

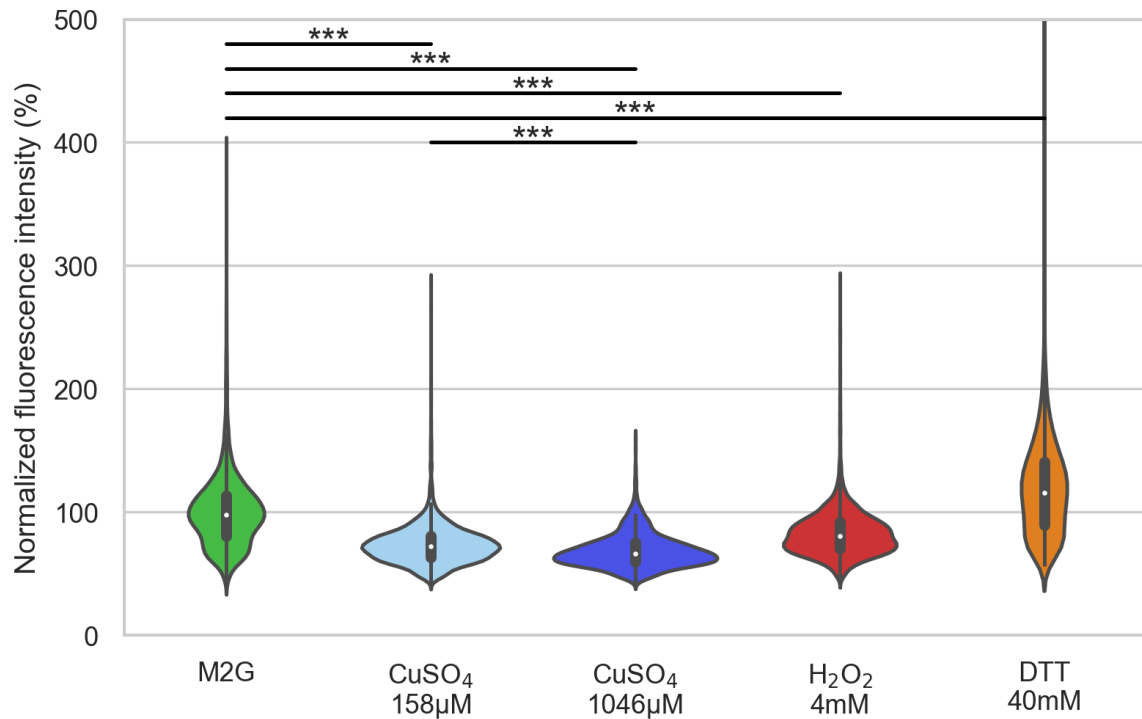


Figure 24: Quantification of the cytoplasmic redox state of CB15N-rxYFP based on microscopy pictures in culture medium (M2G), 158 or 1046 μM copper sulfate (CuSO_4), 4 mM hydrogen peroxide (H_2O_2) or 40 mM Dithioerythiol (DTT) ($\gamma_{\text{ex}} = 512 \text{ nm}$) Violin plot uses a kernel density estimation to show the distribution of the data. Larger portion of the plot represent a higher probability that a bacterium within the population will have on the given Fluorescence intensity. White dot: median. Thick gray: interquartile range. Thin gray line: 95% CI. (M2G: $n_{\text{cells}} = 4552$) (CuSO_4 158 μM $n_{\text{cells}} = 5121$) (CuSO_4 1046 μM : $n_{\text{cells}} = 1900$) (H_2O_2 4 mM $n_{\text{cells}} = 5295$) (DTT 40 mM: $n_{\text{cells}} = 2278$) (One-way ANOVA followed by Tukey comparisons)

RESULT & DISCUSSION

1. Assessment of *in vivo* production of Cu-induced ROS

Previously in the lab, it was shown that *C. crescentus* engages a bimodal response to Cu stress. The ST cell is expelling Cu from its periplasm by a genetically-encoded PcoAB system whereas the SW cell flees away from the Cu source (Lawarée *et al.*, 2016). As Cu might generate a ROS and impact the *C. crescentus* natural redox balance *in vivo*, it was tempting to hypothesize that these ROS might be somehow involved in the Cu flight. The laboratory derivative *C. crescentus* CB15N strain (WT) was used to address this question. First, to determine whether *C. crescentus* is able to flee from putative ROS generated by Cu, it is important to assess whether Cu can generate ROS *in vivo*. A *C. crescentus* strain (WT-rxYFP) constitutively expressing a cytoplasmic intensimetric redox-sensitive yellow fluorescent protein (rxYFP) was used to address this question. Upon oxidation of the rxYFP, the formation of the C149-C202 disulfide bond leads to a decrease of the 512 nm emission peak (Figure 21) (Lukyanov and Belousov, 2014). Therefore, rxYFP can be used *in vitro* and *in vivo* as a sensor of the glutathione oxidative state as it slowly equilibrates with both reduced (GHS) and oxidized glutathione (GSSG) (Lukyanov and Belousov, 2014; Østergaard *et al.*, 2004). *In vivo*, this slow equilibrium is accelerated by the presence of Grx (Lukyanov and Belousov, 2014; Østergaard *et al.*, 2004) Grx are proteins involved in reduction of non-native oxidized Cys residues that might appear when the cells are exposed to an oxidative stress (Ezraty *et al.*, 2017).

The WT-rxYFP fluorescence intensity was monitored over 20 minutes in a poor culture medium (M2G), with either 158 μM and 1046 μM CuSO_4 , 4 mM H_2O_2 or with 40 mM dithiothreitol DTT (Figure 2). H_2O_2 and DTT were used as positive controls for oxidative and reductive conditions, respectively. The two CuSO_4 concentrations correspond to concentrations impacting *C. crescentus* growth in PYE (158 μM) and HIGG (1056 μM) media, respectively.

After 20 minutes, the cells were analyzed by fluorescence microscopy to determine whether the fluorescence intensity was homogeneous within the population (Figures 23, 24). In the fluorometry experiment (Figure 22), the control condition was correct as the overall fluorescence intensity did not vary over time. The addition of H_2O_2 resulted in a drop of the fluorescence intensity whereas the addition of DTT had the opposite effect, indicating that the rxYFP is correctly responding to oxidative and reductive conditions in *C. crescentus*. When exposed to CuSO_4 , CB15N-rxYFP showed a decrease of the fluorescence intensity over time. This decrease seems to be faster with increasing concentrations of CuSO_4 . For the CB15N-rxYFP incubated with 1046 μM CuSO_4 , the fluorescence reached what seems the minimal intensity after 10 minutes, whereas bacteria incubated with 542 μM Cu only reached the minimal fluorescence level after 20 minutes (data not shown). CB15N-rxYFP incubated with only 158 μM CuSO_4 did not reach the same threshold after 20 minutes. It seems that the oxidative impact when adding CuSO_4 to the cells is dose-dependent up to a threshold.

Microscopy analysis was concordant with the fluorometry analysis. As expected DTT increased the overall fluorescence (+20%) whereas H_2O_2 decreased it (-17%) (Figure 23, 24). CuSO_4 -exposed cells tend to have a decrease in the fluorescence intensity compared to the non-exposed cells. Fluorescence within the population seemed rather homogenous. However, the fluorescence intensity for the control M2G condition is more distributed within the population. This might reflect the natural propensity of *C. crescentus* to alter its cytoplasmic redox state along its cell cycle. Addition of CuSO_4 seemed to impact the redox state of *C. crescentus*, suggesting that Cu is able to generate ROS *in vivo*.

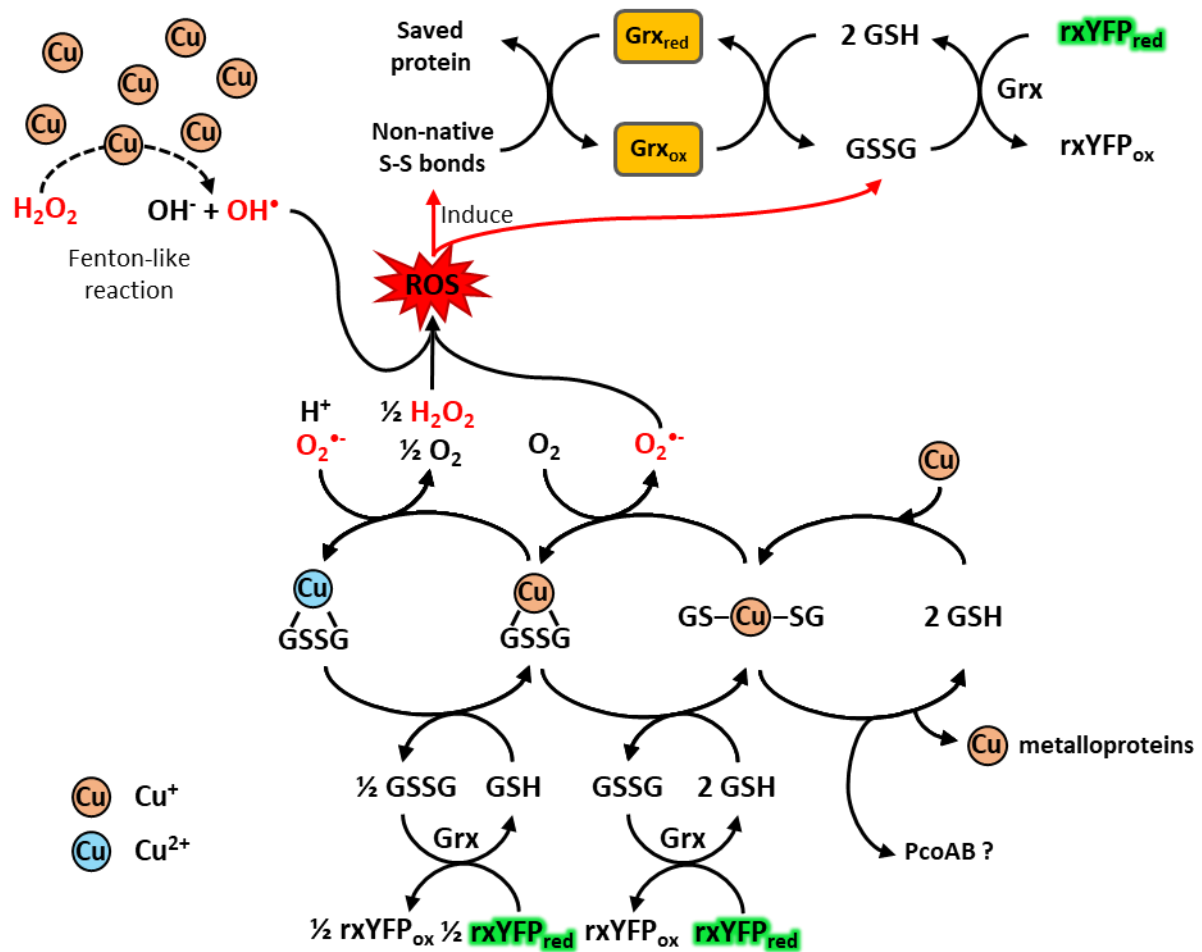


Figure 25: *In vivo* detoxification reactions of Cu⁺ by glutathione, Fenton-like reaction and equilibrium with the redox sensitive yellow fluorescent protein (rxYFP). Red highlight represents oxidants, green highlight represents the fluorescent reduced rxYFP. SOD stands for superoxide dismutase, Grx for Glutaredoxin, GSH for reduced glutathione and GSSG for oxidized glutathione. When Cu⁺ enters *C. crescentus*, it will form a complex with 2 GSH. This complex will be oxidized into a Cu-[GSSG] intermediate to form Cu₂[GSSG]. Cu₂[GSSG] is then able to be regenerated into Cu-[GSH]₂ by reacting with available GSH. This mechanism avoids Cu⁺ to be used as a catalyst in a Fenton-like Haber-Weiss reaction thus producing extremely reactive OH[•]. Cu-[GSH]₂ pool can then be diminished by integrating Cu into Cu containing proteins and/or can be expelled via the PcoAB system when the swarmer cell differentiates into a stalked cell. rxYFP is able to sense the GSH/GSSG ratio in every step of the detoxification. The Fenton-like reaction might happen if the previous mechanism is either defective, saturated or inexistent in *C. crescentus* but it can also be sensed by the rxYFP. Adapted from Aliaga *et al.*, 2012; Freedman *et al.*, 1989; Kimura and Nishioka, 1997; Lawarée *et al.*, 2016; Nies and Herzberg, 2013 and Østergaard *et al.*, 2004. Ezraty *et al.*, 2017)

These Cu-induced ROS might be directly generated through a Fenton-like reaction or through a GSH-mediated Cu detoxification (Figure 25). When Cu^+ enters *C. crescentus*, it might form a complex with 2 GSH. This complex might then be oxidized into a $\text{Cu}^+[\text{GSSG}]$ intermediate to form $\text{Cu}^{2+}[\text{GSSG}]$. $\text{Cu}^{2+}[\text{GSSG}]$ could turn into $\text{Cu}^+[\text{GSH}]_2$ by reacting with available GSH. This mechanism could generate $\text{O}_2^{\cdot-}$ and H_2O_2 but should prevent Cu^+ to be used as a catalyst in a Fenton-like reaction and to produce the extremely reactive OH^{\cdot} . The $\text{Cu}^+[\text{GSH}]_2$ pool can be diminished by integrating Cu^+ into Cu-containing proteins or might be expelled via the PcoAB system when the SW cell differentiates into a ST cell. The basis of this process was already shown as a means for a cell exposed to Cu to avoid generation of highly reactive free OH^{\cdot} (Freedman *et al.*, 1989; Nies and Herzberg, 2013). Even though this process avoids the generation of OH^{\cdot} , it still generates $\text{O}_2^{\cdot-}$ and some H_2O_2 (Freedman *et al.*, 1989; Nies and Herzberg, 2013). In this case, the rxYFP would react to the impact on the GSH caused directly by Cu and indirectly by the putative disulfides bond generated by the produced H_2O_2 and $\text{O}_2^{\cdot-}$. These disulfide bonds could be either directly formed on the GSH pool or formed on some cytoplasmic proteins. Those then might be saved by the activity of one of the *C. crescentus* Grx that would transfer the non-native disulfide bond of the proteins to the GSH pool (Ezraty *et al.*, 2017).

In order to confirm that Cu impacts redox balance *in vivo*, *C. crescentus* sensitivity to Cu was assessed in the presence of anti-oxidant agents. First, assessment of *C. crescentus* WT growth under H_2O_2 was performed as a positive control for oxidative stress (Figure 26). Growth under 40 μM H_2O_2 stress induced a delay in the bacterial exponential growth. Tentative to suppress this delay with the addition of ascorbate were performed. Ascorbate alone was well tolerated by *C. crescentus* up to 0.5 mM, then it started to be deleterious (Figure 27). A hypothesis would be that the addition of too much ascorbate would impair the normal cell cycle-associated redox switch of *C. crescentus* (Narayanan *et al.*, 2015). This would lock the cell cytoplasm into a reduced state. This reduced state would be a problem for the stalked cell. Indeed, this morphotype is normally in a more oxidized state, allowing the correct synthesis of dNTPs through the RNR. If this cell type is locked in a more reduced state this might impair the correct regeneration of the RNR redox state and thus its activity (Goemans *et al.*, 2018). The addition of 0.1 to 0.5 mM of ascorbate to 40 μM H_2O_2 successfully saved *C. crescentus* (Figure 28). However, ascorbate was unable to save *C. crescentus* from Cu stress (Figure 29). The addition of ascorbate to cells exposed to Cu stress was even more deleterious than Cu stress alone. Even if ascorbate is able to prevent oxidative stress, it also seems to be able to react with Cu and to induce a pro-oxidant effect (Zhou *et al.*, 2016). It seems that the addition of anti-oxidant is not an adequate solution to mitigate the Cu-induced ROS.

An alternative strategy is to measure the Cu sensitivity of various KO mutants related to natural anti-oxidant defenses such as the sole catalase-peroxidase *katG* and the cytoplasmic superoxide dismutase *sodA*, which is the first SOD to be upregulated when *C. crescentus* is exposed to heavy metals (Hu *et al.*, 2005). Accordingly, *sodA* has been recently isolated in the lab in a genetic screen seeking for more sensitive Cu mutants. Clean *sodA* and *sodB* KO mutants were successfully constructed. ΔsodA was confirmed to be more sensitive to Cu (Figure 30). On the other hand, ΔsodB does not seem to impact the growth of *C. crescentus* (Figure 31). As mentioned before, *sodA* is upregulated in most heavy metals stress whereas *sodB* was only upregulated with a very high concentration of Cd (Hu *et al.*, 2005). This suggests a backup role of *sodB*. This also tends to confirm that Cu could indeed be a source of ROS *in vivo*. In this purpose, it might be interesting to assess the cytoplasmic redox state KO and overexpression mutants upon Cu stress to see whether those genes are somehow involved in Cu defense by diminishing the oxidative stress part.

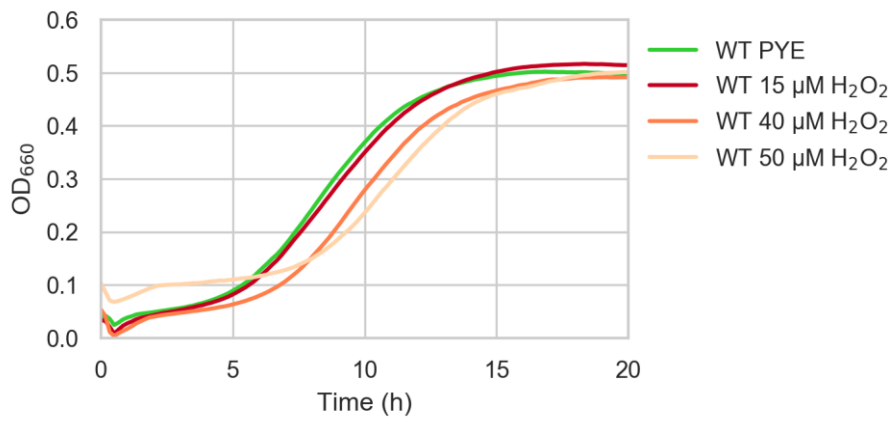


Figure 26: Growth curves of WT *C. crescentus* in PYE rich media with different concentrations of H_2O_2 (biological replicates = 3; technical replicates = 3)

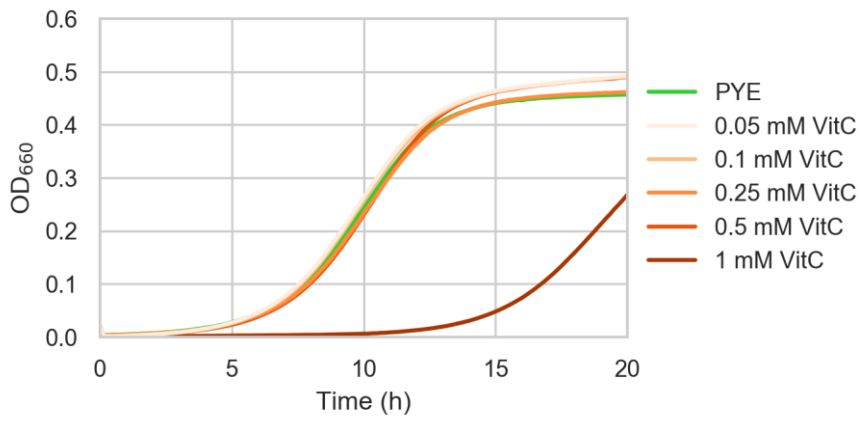


Figure 27: Growth curves of WT *C. crescentus* in PYE rich media with different concentrations of ascorbate (VitC) (biological replicates = 3; technical replicates = 3)

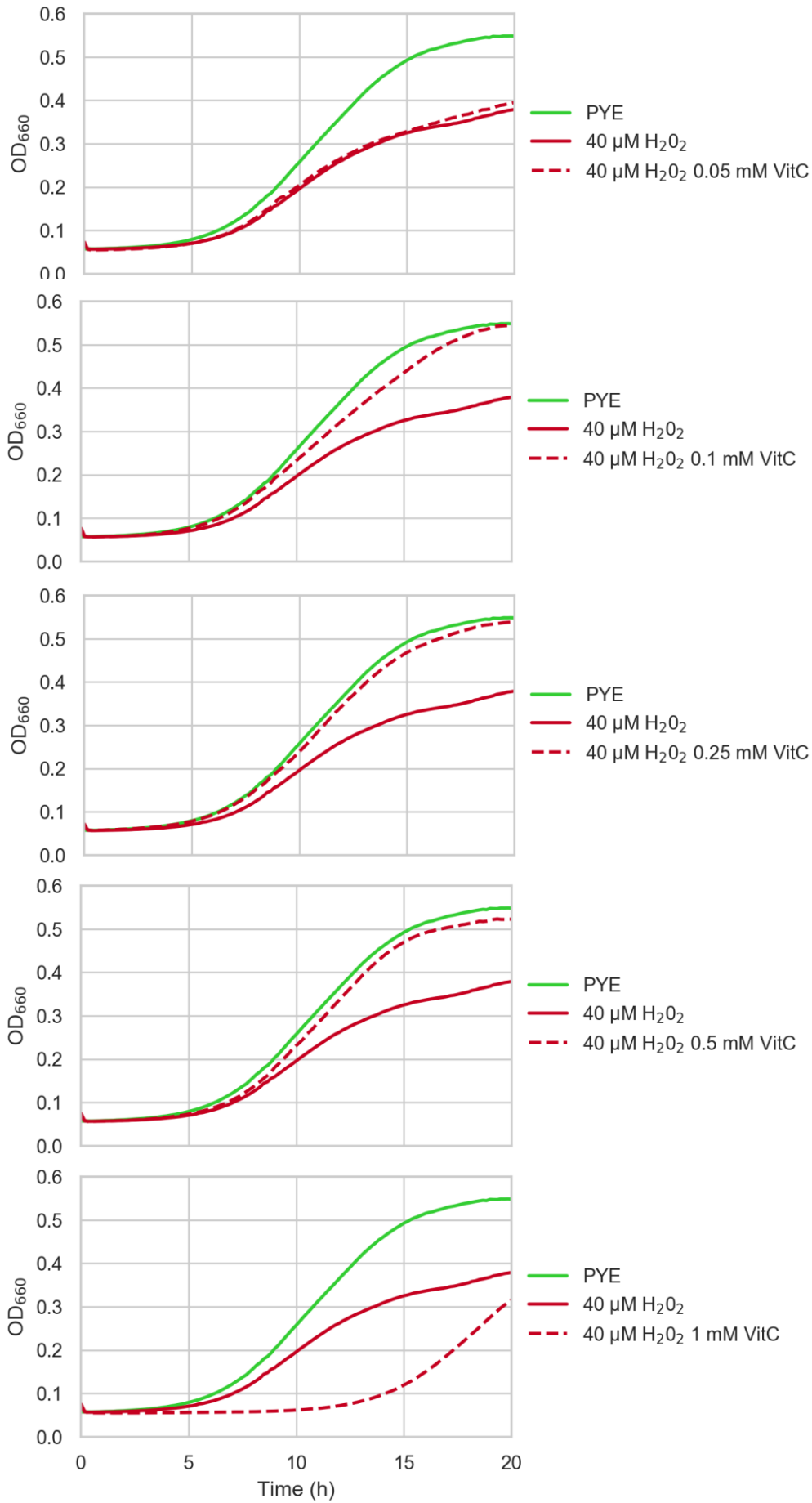


Figure 28 : Growth curves of WT *C. crescentus* in PYE rich media with or without 40 μM H₂O₂, with different concentrations of ascorbate (VitC) (biological replicates = 3; technical replicates = 3)

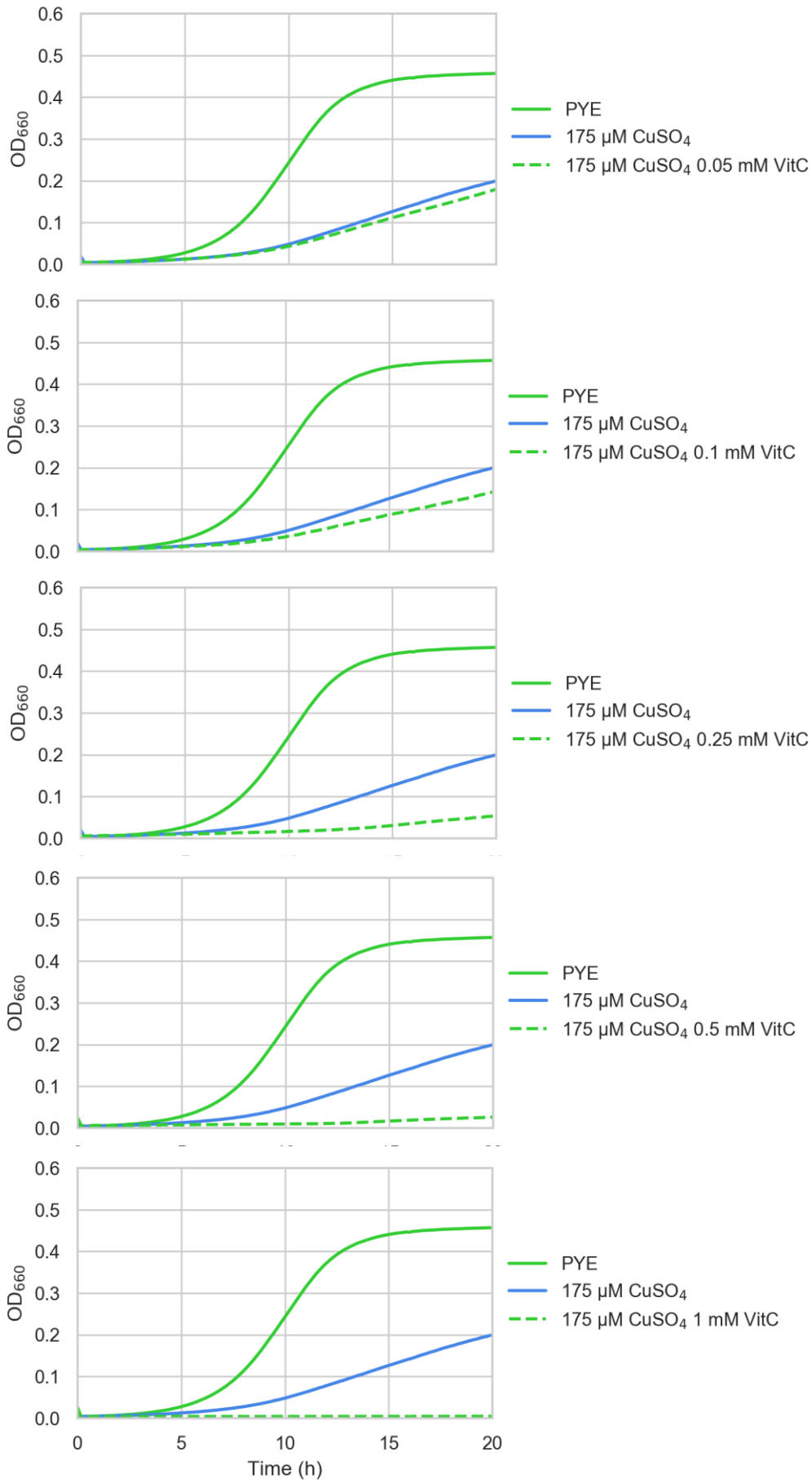


Figure 29 : Growth curves of WT *C. crescentus* in PYE rich media with or without 175 μM CuSO₄, with different concentrations of ascorbate (VitC) (biological replicates = 3; technical replicates = 3)

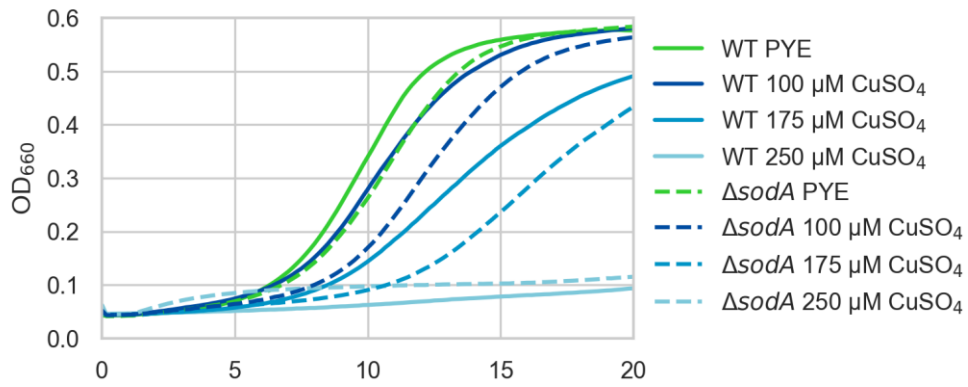


Figure 30: Growth curves of *C. crescentus* CB15N Δ sodA compared to *C. crescentus* CB15N WT in PYE rich media with different concentrations of CuSO₄ (biological replicates = 2; technical replicates = 3)

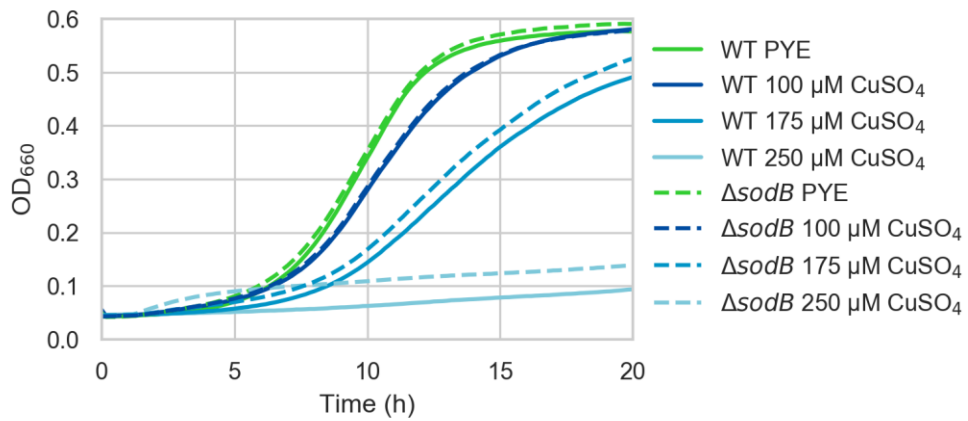


Figure 31: Growth curves of *C. crescentus* CB15N Δ sodB compared to *C. crescentus* CB15N WT in PYE rich media with different concentrations of CuSO₄ (biological replicates = 2; technical replicates = 3)

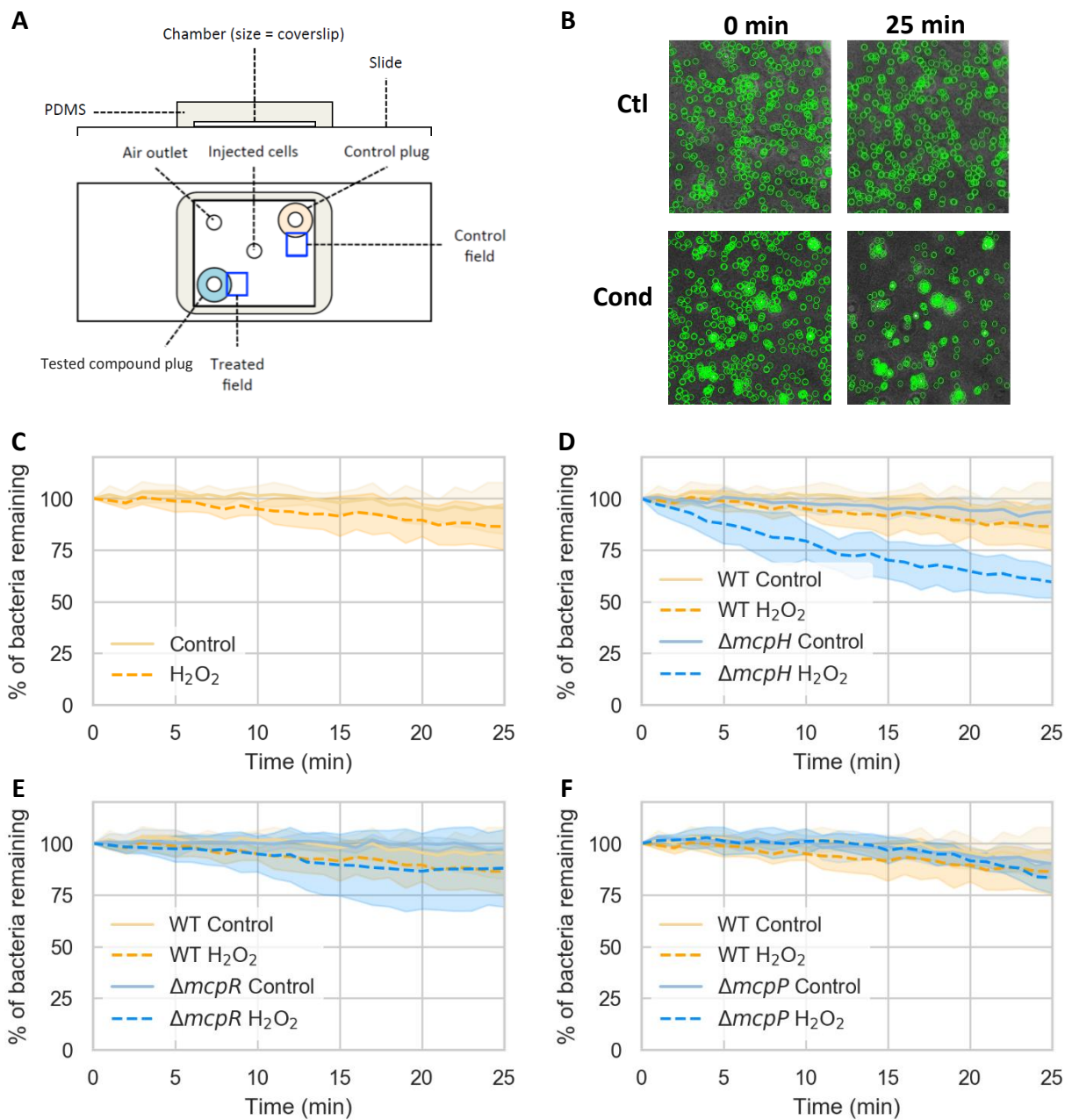


Figure 32: **A.** Schematic representation of the PDMS device. Adapted from Lawarée *et al.*, 2016. **B.** Typical pictures obtained after an LCI experiment with flight under the tested condition (Cond). **C.** WT SW exposed to 40 μM H_2O_2 (biological replicates = 3). **D.** $\Delta mcpH$ SW exposed to 40 μM H_2O_2 (biological replicates = 3). **E.** $\Delta mcpR$ SW exposed to 40 μM H_2O_2 (biological replicates = 4). **F.** $\Delta mcpP$ SW exposed to 40 μM H_2O_2 (biological replicates = 3).

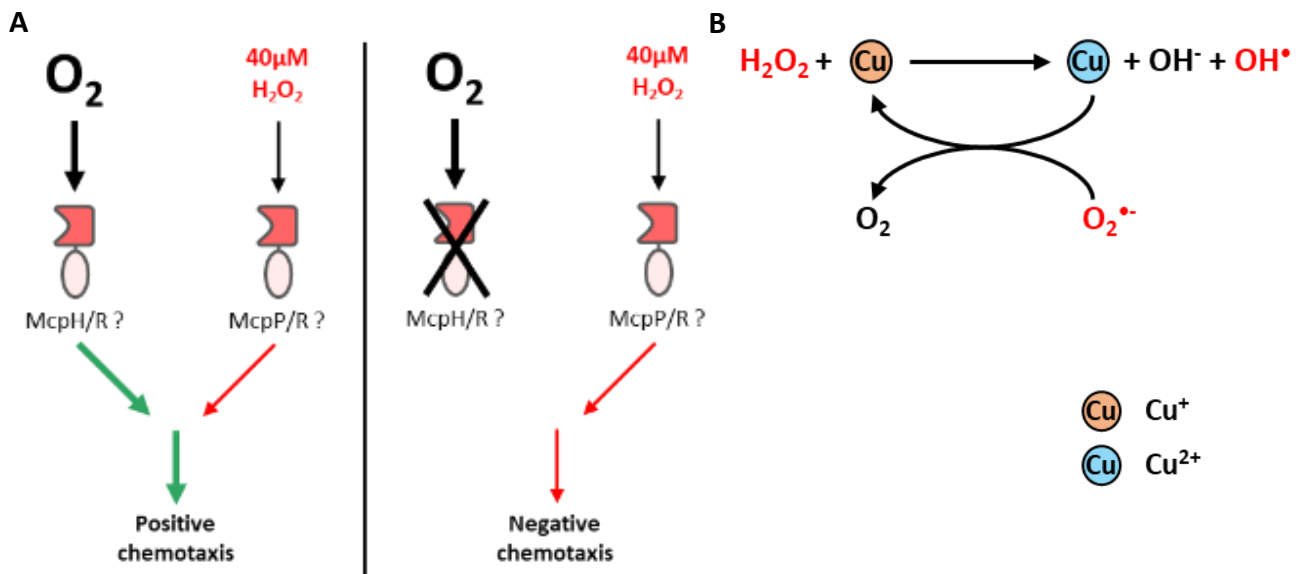


Figure 33: **A.** Potential Interplay between the positive oxygen chemotaxis and the negative H₂O₂ chemotaxis. **B.** Origin of O₂ by the Haber-Weiss cycle.

2. Impact of ROS on *C. crescentus* chemotaxis

Single KO mutants of every *C. crescentus* MCPs have been realized in the context of Gwennaëlle Louis' thesis and their chemotaxis toward Cu was tested by live chemotaxis imaging (LCI). Briefly, isolated *C. crescentus* SW cells are injected in a small chamber where two agarose plugs were previously molded in two opposites corners of the chamber: a control plug and a plug with a determined concentration of the tested compound (Figure 32A). Pictures are taken over a given time period in the vicinity of the two plugs (Figure 32A, B). This allows the identification of *mcpH*, *mcpP*, *mcpR*, *mcpC*, and *mcpG* as putative MCPs involved in Cu sensing.

As Cu might impact the *C. crescentus* normal redox balance, it was then interesting to determine whether one of the MCP candidates described above could sense the putative Cu-induced ROS. At first, H₂O₂ was tested as a putative chemorepellent against those MCPs. The idea was that H₂O₂ would react with cytoplasmic free Fe in a Fenton reaction to somehow mimic the putative Fenton-like reaction that could happen with Cu. This idea was further motivated by the fact that in *H. pylori*, the addition of either Fe or H₂O₂ seemed to induce a flight to the Fenton generated ROS (Collins *et al.*, 2016). So by adding either Cu and thus provoking a Fenton-like reaction or H₂O₂, provoking Fenton reactions, *C. crescentus* should flee in both cases.

Analysis of the first LCI results seemed to indicate a flight of *C. crescentus* cells from 40 μM H₂O₂ (Figure 32C), but more in-depth analysis revealed issues in these experiments. Classical issues and possible improvements of LCI experiments will be discussed later.

Even if the WT cells do not fly from 40 μM H₂O₂, Δ *mcpH* mutant displayed a significant flight from H₂O₂ (Figure 32D) whereas Δ *mcpR* was fleeing in half of the experiments (Figure 32E). Interestingly, McpH and McpR exhibit PAS domains in their predicted ligand binding domains. PAS domains are well known to sense a lot of chemical cues, often associated with redox state or O₂ (Ortega *et al.*, 2017). As *C. crescentus* display a positive chemotaxis toward O₂ (Morse *et al.*, 2016), it would not be surprising that at least McpH and/or McpR is involved in O₂ sensing (Figure 33A). An excess O₂ near the H₂O₂ plug may originate from H₂O₂ itself (Figure 33B). Indeed, as the LCI PDMS devices are reused for multiples experiments, it might be possible that some residual Cu remains in holes used to mold the H₂O₂ plug. If this assumption is correct it would not be surprising for O₂ to be formed by a Fenton-like Haber-Weiss reaction with Cu. This would lead to an increase in the O₂ concentration and a decrease in H₂O₂ concentration (Figure 33B). This will lead the cell in a rather positive or neutral chemotaxis as the O₂ attraction and the H₂O₂ repulsion inhibit each other. So, when one of those two MCPs is removed, the cell lost its ability to sense O₂ to only sense the H₂O₂, inducing a flight response (Figure 33A). However, the MCP(s) responsible involved in H₂O₂ sensing remain(s) to be determined. As the WT is not fleeing from 40 μM H₂O₂ (Figure 32C), it is impossible to detect mutants with decreased flight. It would be interesting to test whether a higher concentration of H₂O₂ can induce a flight in the WT strain. This might allow determining whether one of the remaining candidates do not flee at a concentration where the WT does. If interesting candidates are isolated with a reduced H₂O₂ flight, it might be useful to test them for Fe chemotaxis. Indeed, similarly to what is thought to happen when adding H₂O₂, adding Fe should also promote cytoplasmic Fenton reactions. This would be a great way to compare what would happen with a Cu-induced Fenton like reaction.

Interestingly, Δ *mcpG* mutant flees from both the control and the H₂O₂ plug (Figure 34), similarly to what was observed in the Cu experiment (Gwennaëlle Louis' thesis). MCPs are organized within huge clusters capable of readily amplify a signal (Collins *et al.*, 2014; Parkinson *et al.*, 2015; Salah Ud-Din and Roujeinikova, 2017). If McpG is one of the main

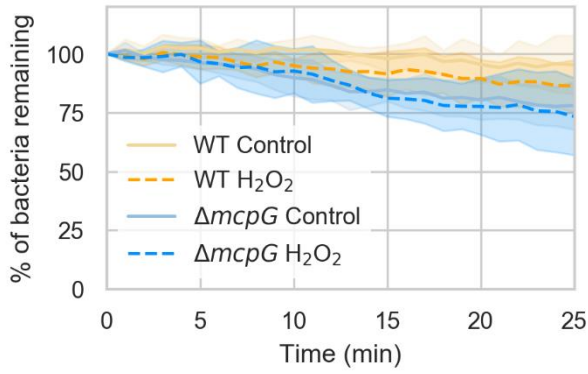


Figure 34: $\Delta mcpG$ SW exposed to 40 μM H_2O_2 (biological replicates = 3).

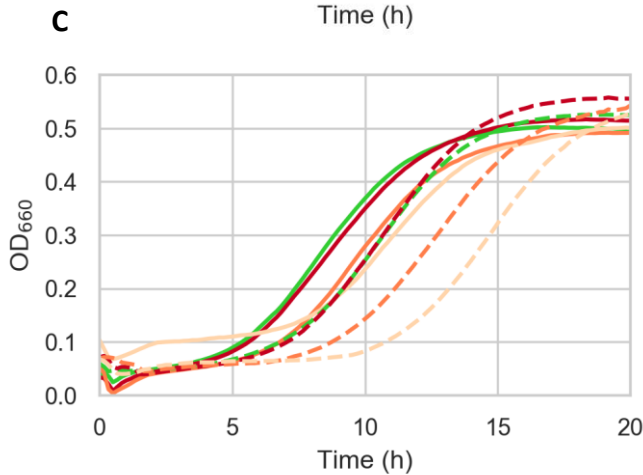
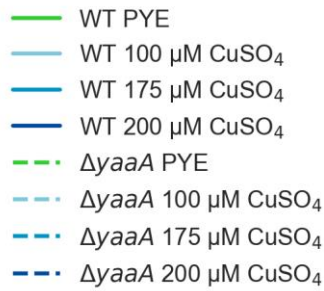
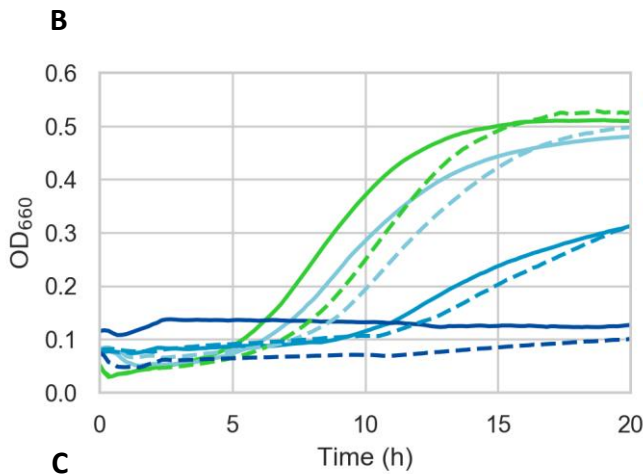
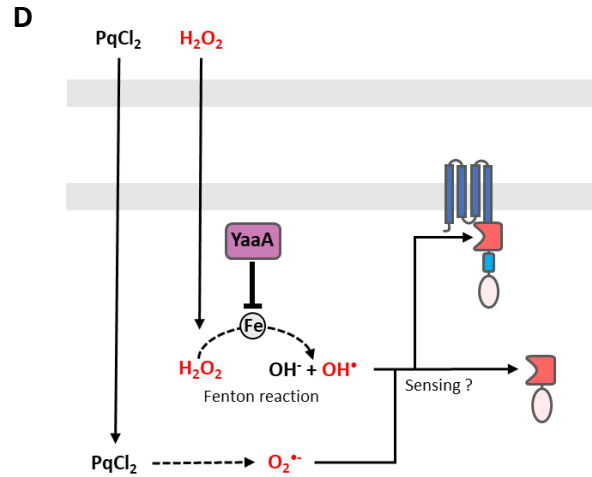
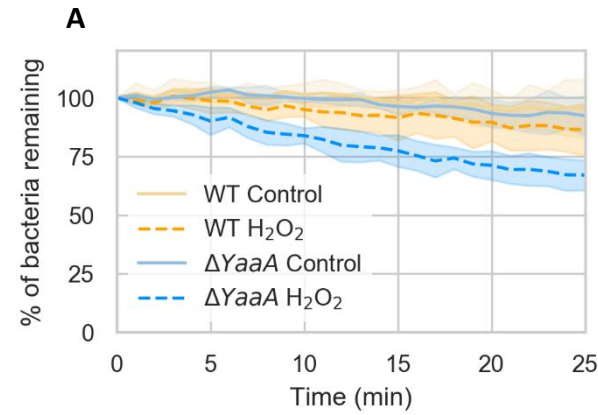


Figure 35: **A.** $\Delta yaaA$ SW exposed to 40 μM H_2O_2 (biological replicates = 3). **B.** Growth curves of $\Delta yaaA$ compared to *C. crescentus* CB15N WT *C. crescentus* CB15N WT in PYE rich media with different concentrations of CuSO_4 (biological replicates = 3; technical replicates = 3). **C.** Growth curves of $\Delta yaaA$ compared to *C. crescentus* CB15N WT *C. crescentus* CB15N WT in PYE rich media with different concentrations of H_2O_2 (biological replicates = 3; technical replicates = 3) **D.** Model of the impact of YaaA on H_2O_2 sensing. YaaA inhibits the Fenton reaction by sequestering the free Fe ions thus reducing the number of OH^\cdot that might be sensed by an MCP. Full arrows: displacement of a given compound. Dashed arrows: Transformation of a given compound.

MCP constituting these clusters, its deletion could have drastic consequences on chemotaxis. The $\Delta mcpG$ mutant might be unable to correctly regulate the flagellar rotation, transforming the biased walk that is chemotaxis into a more random walk, explaining the behavior of this strain in LCI.

A genetic screen seeking for *C. crescentus* mutants with altered Cu chemotaxis led to the identification of *yaaA* (Pauline Cherry master thesis). *E. coli* YaaA is thought to reduce free cytoplasmic Fe upon H₂O₂ stress to avoid Fenton-reactions (Liu *et al.*, 2011). Clean KO mutant of *yaaA* in *C. crescentus* showed a growth defect under control conditions, which was amplified upon H₂O₂ stress but not upon Cu stress (Figure 35B, C). In *E. coli*, *yaaA* expression is induced under strong H₂O₂ stress only. However, *C. crescentus* presents a basal *yaaA* expression level, suggesting that *yaaA* might be more important in *C. crescentus* than in *E. coli*. In LCI, *C. crescentus* $\Delta yaaA$ showed an increased flight from H₂O₂ compared to the WT strain (Figure 35A). The absence of *yaaA* could potentially increase the intracellular level of free Fe and in turn the level of cytoplasmic OH[•] through Fenton reactions (Figure 35D). If OH[•] is sensed by an MCP, a situation similar to what could be hypothesized in *H. pylori* would be observed. In *H. pylori*, cytoplasmic chemoreceptor TlpD is able to sense Fenton reaction-induced ROS (Collins *et al.*, 2016). If an MCP is able to sense the OH[•] produced by a Fenton reaction, *yaaA* KO would result in an increased flight as its deletion might promote Fenton reactions. In growth curves, this would result in an increased H₂O₂ toxicity. To further test whether *C. crescentus* is able to sense Fenton induced ROS, two main approaches could be investigated after finding an appropriate H₂O₂ concentration leading to a WT flight: either overexpressing *C. crescentus* catalase-peroxidase *katG* to reduce intracellular H₂O₂ or chelating the intracellular Fe like it was done in *H. pylori*. However, the second approach might be difficult to perform as it was recently shown that Fe deprivation in *C. crescentus* increases the intracellular concentration of H₂O₂ by an unknown mechanism (Leaden *et al.*, 2018).

Consistent with the hypothesis that there might be at least one MCP able to sense cytoplasmic ROS, the WT strain flees from 30 μ M PqCl₂ (Figure 36B). PqCl₂ is a potent herbicide able to generate mostly intracellular O₂^{•-} (Hassan and Fridovich, 1979) thus potentially making it a better substitute than H₂O₂ to mimic the effects of the putative *in vivo* Cu-induced ROS. However, even if this concentration is toxic for *C. crescentus* and reduces its growth rate (Figure 36A), it does not seem to readily impact the GSH/GSSG equilibrium in fluorometry experiments like it is the case with CuSO₄ (data not shown). However, a slight decrease (-6%) can be observed by quantifying the microscopy images (Figure 36C). It is highly probable that this concentration of PqCl₂ does not have a huge impact on the cellular redox state over a small period of time. This assesses a need for *C. crescentus* to sense ROS before they are able to generate an oxidative stress. Indeed, as the SW cell type is associated with a more reduced cytoplasmic redox state (Narayanan *et al.*, 2015). So, even a small amount of ROS might impact its normal development. To counteract that, the SW cell would need of early detection of pro-oxidative environment to readily induce a flight response.

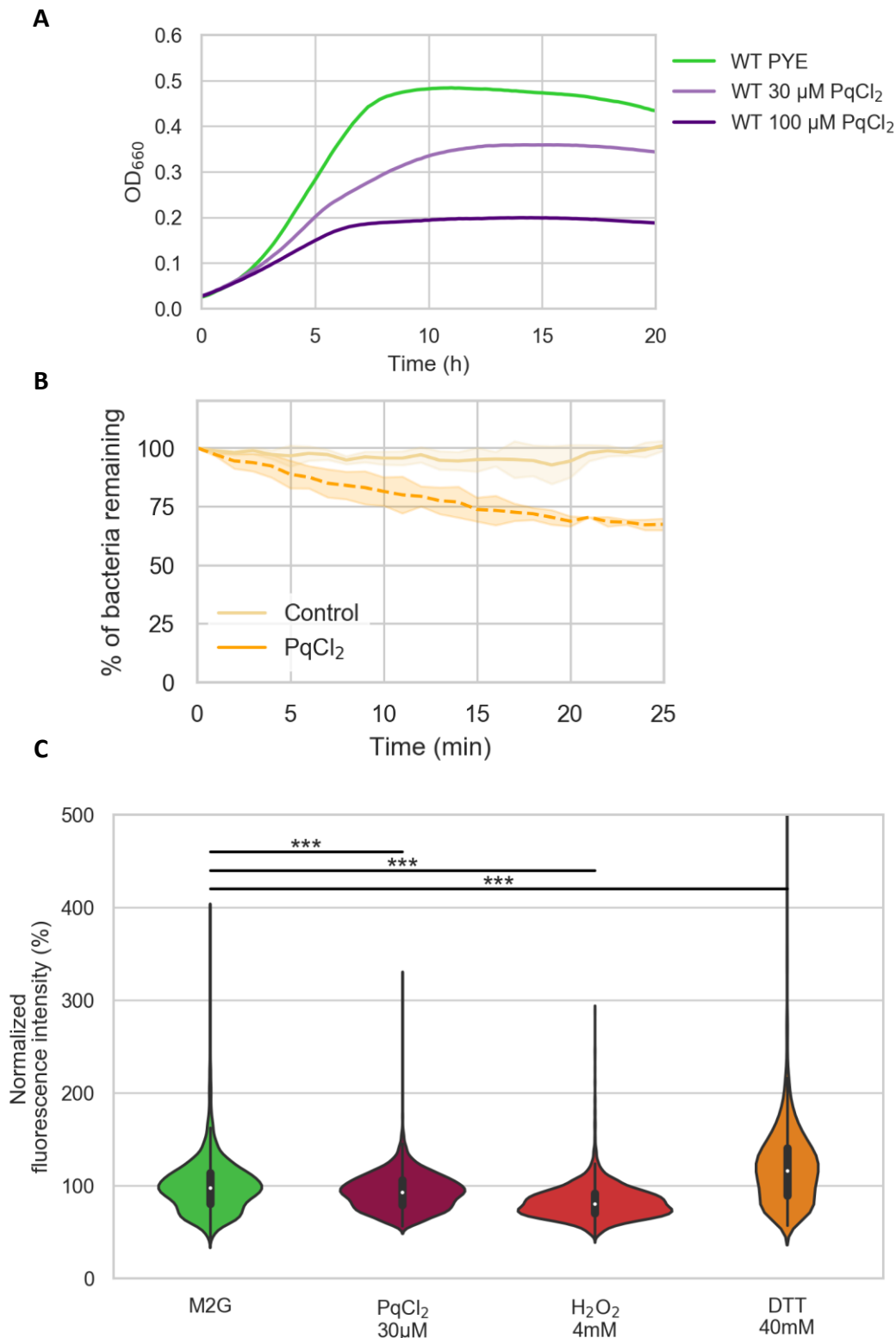


Figure 36: **A.** Growth curves *C. crescentus* CB15N WT in PYE rich media with different concentrations of CuSO₄ (biological replicates = 2; technical replicates = 3) **B.** WT SW exposed to 30 μ M PqCl₂ (biological replicates = 3). **C.** Quantification of the cytoplasmic redox state of CB15N-rxYFP based on microscopy pictures in culture medium (M2G), with 30 μ M paraquat dichloride (PqCl₂), 4 mM hydrogen peroxide (H₂O₂) or 40 mM dithioerythiol (DTT) ($\gamma_{\text{ex}} = 512$ nm) Violin plot use a kernel density estimation to show the distribution shape of the data. Larger portion of the plot represent a higher probability that a bacterium within the population will have on the given Fluorescence intensity. White dot: median. Thick gray: interquartile range. Thin gray line: 95% CI. (M2G: $n_{\text{cells}} = 4552$) (PqCl₂ 30 μ M: $n_{\text{cells}} = 3067$) (H₂O₂ 4 mM $n_{\text{cells}} = 5295$) (DTT 40 mM: $n_{\text{cells}} = 2278$)

3. Issues and potential improvements of LCI

LCI is a relatively new experiment and might be sensitive to some issues. During this master thesis, a lot of experiments had to be aborted or discarded. So, a clear understanding of those issues and how to prevent them might help to improve this experiment. First, for convenience, PDMS devices are reused between experiments. During the firsts LCI experiments with almost exclusively Cu, this was not posing detectable problems. However, with the use of a compound that could react with Cu, this might pose a problem if between experiments some trace of Cu remains in the PDMS. H_2O_2 might react with this remaining Cu and form active OH^\cdot that would probably never reach the cells due to their low stability. Another issue with the remaining Cu is that the uses of the two plugs might differ between experiments. A hole previously used as a Cu plug could be used as a control plug in another experiment. This might induce a slight flight from the control plug forcing to discard the experiment. Leaks in the device might also happen to cause flow in the area checked for flight thus conducting to false positives or flight near the control plug forcing the experiment to be discarded. The ideal solution would be to use a new PDMS device for every experiment and to seal them with plasmas cleaning or thermal bonding to avoid any leak. However, this method would be tedious and more expensive. A simpler alternative would be to split PDMS device along the compound used and to mark the control plug to always reuse the same.

Currently, 10 pictures on the Z-axis are taken at a regular interval between the two extremes positions where bacteria could be detected. As often we could only detect the flight from only one Z-axis, we can wonder whether sometimes the flight was missed because the interval was set too high due to more extremes position of the bacteria. So, starting to use the same interval, even if sometimes increase the number of pictures and thus the analysis time, could help detect the flight where it could have been missed sometimes.

CONCLUSION & PERSPECTIVES

Our analysis with the redox-sensitive rxYFP tends to confirm that Cu might impact the normal *C. crescentus* redox balance. Furthermore, SodA was identified and confirmed to have an impact on growth upon Cu stress, suggesting that Cu might indeed produce ROS in vivo. This would explain the impact on the redox balance. However, the mechanism by which those ROS are generated is not clear. They can happen either by the glutathione-mediated Cu-detoxification or by Fenton-like reactions. An involvement of a Fenton reaction from the Fe ions coming from the displaced Fe-S cluster is not to be excluded. With the advancements in ROS specific probes (Bilan et al., 2013; Lei et al., 2017; Lu et al., 2017) it might be possible to identify which ROS are generated in *C. crescentus* upon Cu stress and thus the mechanism involved in their generation.

Even if the attempts to suppress the oxidative stress part of Cu toxicity with a natural antioxidant like the ascorbate were rather unsuccessful, mutants surexpressing *C. crescentus* catalase and/or superoxide dismutases remains to be tested. This will help to confirm the nature of the ROS as well as their contribution in the Cu toxicity.

Then, we have shown that *C. crescentus* is able to flee from oxidative stress generated by 30 μM PqCl_2 , even if its impact on the redox balance is rather limited. This led to the hypothesis that the redox state of *C. crescentus* might be so important for its cell cycle that *C. crescentus* SW cells must readily engage a flight response upon oxidative stress sensing. In this context, it would make sense for the oxidative stress response to also be bimodal. Indeed, it has recently been shown that Trx1, the sole Trx in *C. crescentus* is only expressed during the ST cell phase. One could hypothesize that Trx1 would be one of the major actors for the ST cell defense against oxidative stress (Goemans et al., 2018) whereas the SW cell readily engage a flight response upon ROS detection.

Although WT strain does not seem to flee from 40 μM H_2O_2 , some mutants were able to. This suggested a putative opposition with a positive chemotaxis, potentially toward O_2 . As experiments to detect O_2 chemotaxis in *C. crescentus* exist, it would be interesting to test ΔmcpH and ΔmcpR in those experiments. ΔyaaA was also presenting a flight from H_2O_2 . This suggested a more important role of this protein toward H_2O_2 stress in *C. crescentus* than in *E. coli*. Future works with higher concentrations of H_2O_2 would be needed to find one where the WT strain does not fly. This would allow the identification of putative mutants with a reduced H_2O_2 flight. LCI with a metal known to induce oxidative stress (Fe), or not (Zn) would also help determine if oxidative stress is involved in the flight mechanism.

Table 1: Strains and plasmids used in this work

| Strain | Description |
|-----------------------|---|
| <i>C. crescentus</i> | |
| CB15N | Laboratory variant of CB15 strain, easily synchronizable |
| CB15N-rxYFP | CB15N constitutively expressing rxYFP |
| <i>ΔmcpH</i> | CB15N <i>ΔmcpH</i> |
| <i>ΔmcpP</i> | CB15N <i>ΔmcpP</i> |
| <i>ΔmcpR</i> | CB15N <i>ΔmcpR</i> |
| <i>ΔmcpG</i> | CB15N <i>ΔmcpG</i> |
| <i>ΔsodA</i> | CB15N <i>ΔsodA</i> |
| <i>ΔsodB</i> | CB15N <i>ΔsodB</i> |
| <i>ΔyaaA</i> | CB15N <i>ΔyaaA</i> |
| <i>E. coli</i> | |
| DH10B Helper | Helper strain for the tri-parental mating |
| DH10B pNPTS | Strain used to construct the K-O mutants by tri-parental mating |
| Plasmid | |
| <i>pNPTS</i> | Deletion vector, KmR, sacB |
| <i>pBXMCS2::rxYFP</i> | Plasmid used for constitutive expression of rxYFP |

METHODS

Bacterial strains & plasmids

C. crescentus strains were grown at 30°C in Peptone Yeast Extract (PYE) rich medium (see Table 2 for composition) (Ely, 1991) or M2-Glucose (M2G) minimal medium (see Table 3 for composition) supplemented by 5 µg.ml⁻¹ kanamycin when required. *E. coli* strains were grown at 37°C in LB (Luria-Bertani) (see Table 4 for composition). Plasmids were mobilized from *E. coli* DH10B or into *C. crescentus* by conjugation. All strains and plasmid used are listed in Table 1. Cultures in exponential growth phase were used in every experiment.

Knock-out mutant construction

One gBlock[®] Gene Fragment (Integrated DNA technologies) was designed for *sodA sodB* and *yaaA* genes. Each gBlock[®] contains the ~200 bp upstream region of one gene followed by the ~200 bp downstream region of the same gene. These gBlocks[®] were inserted into an EcoRV-linearized pNPTS138 plasmid. The ligation product was transformed into the competent DH10B *E. coli* strain. A tri-parental mating was then performed between the previously transformed DH10B *E. coli* strain, an *E. coli* Helper strain and the WT *C. crescentus* strain.

Clones with the integrated plasmid (the clones that underwent the first homologous recombination event) were selected on a kanamycin-containing medium. A second homologous recombination event was carried out by growing the kanamycin resistant clones without selection pressure and selection for this event was performed by then plating these clones on PYE-3% sucrose plates. This select clones who have lost the plasmid. These clones can be either a clean knock-out strain or a WT strain. The distinction between these two was made by performing a diagnostic PCR (hybridization of chromosomal DNA, ~500-1000 bp from each side of the gene)

Synchrony

C. crescentus swarmer cells are isolated by centrifugation in a silicate gradient as described by (Evinger and Agabian, 1977)

Growth curves determination

Exponential growth phase *C. crescentus* in PYE is added in a 96 well plate (well final volume = 200 µl; well final OD₆₆₀ = 0.05) with the appropriate concentration of CuSO₄, H₂O₂, Paraquat dichloride, DTT or ascorbic acid to be tested. 96 well plate is incubated at 30°C under constant agitation. OD₆₆₀ is measured every 15 minutes for 24 h using an Epoch 2 Microplate Spectrophotometer (BioTek)

Microscopy

Fluorescence and phase contrast microscopy were performed on a Zeiss Axio Imager Z1 equipped with a Hamamatsu Digital Camera C11440 with a 100x PH3 objective. Bacteria were placed on a 1 % agarose PBS pad for imaging. Images were captured and processed with ZEN 2.5 (Carl Zeiss Microscopy GmbH) software. Images were analyzed with Oufi (Paintdakhi *et al.*, 2016) and MATLAB software (MathWorks).

Table 4 : Composition of PYE (Peptone Yeast Extract) rich medium

| PYE | |
|---------------|------------------------|
| Concentration | Compound |
| 0.2 % | Bacto Peptone |
| 0.1 % | Yeast Extract |
| 1 mM | MgSO ₄ |
| 0.5 mM | CaCl ₂ |
| 1.5 % | Agar (for solid media) |

Table 3 : Composition of M2G (M2 salts Glucose) poor medium

| M2G | |
|---------------|----------------------------------|
| Concentration | Compound |
| 6.1 mM | Na ₂ HPO ₄ |
| 3.9 mM | KH ₂ PO ₄ |
| 9.3 mM | NH ₄ Cl |
| 10 μM | FeSO ₄ |
| 10 μM | EDTA |
| 0.5 mM | MgSO ₄ |
| 0.5 mM | CaCl ₂ |
| 0.2 % | Glucose |

Table 2 : Composition of LB (Luria-Bertani) rich medium

| LB | |
|---------------|------------------------|
| Concentration | Compound |
| 1% | Bacto Peptone |
| 0.5 % | Yeast Extract |
| 1% | NaCl |
| 1.5 % | Agar (for solid media) |

Fluorometry

Fluorometry was performed on a Spectramax ID3 (Molecular Device). Optimal signal to noise ratio wavelengths was selected using the integrated software. The rxYFP fluorescent probe was excited at a wavelength of 509 nm and fluorescence intensity was measured at 545 nm. 200 μ l of bacteria in M2G were incubated at 30°C, under continuous shaking, with the appropriate concentrations of the compounds to test.

Live chemotaxis imaging

The live chemotaxis imaging experiments were adapted from Lawarée *et al.*, 2016. Chemotaxis devices were made by casting solubilized 10:1 polydimethylsiloxane (PDMS Slygard 184, Dow Corning) in a small glass pot (d = 50 mm, h = 30 mm; glassware from Lenz Laborglass Instrument) where coverslips had previously been placed in order to mold the future bacterial chambers. After a degassing phase, the mixed PDMS was heated for 1 h at 70 °C. Unmolded PDMS devices were then mounted on a microscope glass slide. The slide and the PDMS cube were washed successively with acetone (only the slide), isopropanol and methanol and rinsed with milli-Q water. Both components were blown dry between each wash. Three inlets and one outlet channels were drilled in the PDMS, which was then firmly pressed against the slide to seal the device. Melted 1.5% agarose H₂O (10 μ l) with or without 1.16 mM CuSO₄, 40 μ M H₂O₂ or 30 μ M PqCl₂ was loaded into the chamber through both external inlet channels to generate the plugs. Isolated SW cells (150 μ l, OD_{660nm} = 0.01) were, in turn, injected into the bacterial chamber through the central inlet channel. Images were collected every minute for 25 min in one focal plan in the vicinity of the Cu or the control plug with a Nikon Ti-2 Eclipse inverted microscope equipped with a Hamamatsu Digital Camera C13440 with a 20x PH1 objective. All image capture and processing were performed with NIS-Element AR Analysis 5.02.00 software. Quantitative analysis of time-lapse images was performed with MATLAB software (MathWorks).

REFERENCES

- Abreu, I.A., and Cabelli, D.E. (2010). Superoxide dismutases—a review of the metal-associated mechanistic variations. *Biochim. Biophys. Acta BBA - Proteins Proteomics* 1804, 263–274.
- Ahemad, M. (2012). Implications of bacterial resistance against heavy metals in bioremediation: a review. *J. Inst. Integr. Omics Appl. Biotechnol. IIOAB* 3, 9.
- Alexandre, G. (2010). Coupling metabolism and chemotaxis-dependent behaviours by energy taxis receptors. *Microbiology* 156, 2283–2293.
- Amin, M., Kothamachu, V.B., Feliu, E., Scharf, B.E., Porter, S.L., and Soyer, O.S. (2014). Phosphate Sink Containing Two-Component Signaling Systems as Tunable Threshold Devices. *PLoS Comput. Biol.* 10, e1003890.
- Behrens, W., Schweinitzer, T., McMurry, J.L., Loewen, P.C., Buettner, F.F.R., Menz, S., and Josenhans, C. (2016). Localisation and protein-protein interactions of the *Helicobacter pylori* taxis sensor TlpD and their connection to metabolic functions. *Sci. Rep.* 6.
- Bilan, D.S., Pase, L., Joosen, L., Gorokhovatsky, A.Y., Ermakova, Y.G., Gadella, T.W.J., Grabher, C., Schultz, C., Lukyanov, S., and Belousov, V.V. (2013). HyPer-3: A Genetically Encoded H₂O₂ Probe with Improved Performance for Ratiometric and Fluorescence Lifetime Imaging. *ACS Chem. Biol.* 8, 535–542.
- Bondarczuk, K., and Piotrowska-Seget, Z. (2013). Molecular basis of active copper resistance mechanisms in Gram-negative bacteria. *Cell Biol. Toxicol.* 29, 397–405.
- Chaturvedi, K.S., and Henderson, J.P. (2014). Pathogenic adaptations to host-derived antibacterial copper. *Front. Cell. Infect. Microbiol.* 4.
- Chaturvedi, K.S., Hung, C.S., Crowley, J.R., Stapleton, A.E., and Henderson, J.P. (2012). The siderophore yersiniabactin binds copper to protect pathogens during infection. *Nat. Chem. Biol.* 8, 731–736.
- Chaturvedi, K.S., Hung, C.S., Giblin, D.E., Urushidani, S., Austin, A.M., Dinauer, M.C., and Henderson, J.P. (2014). Cupric Yersiniabactin Is a Virulence-Associated Superoxide Dismutase Mimic. *ACS Chem. Biol.* 9, 551–561.
- Collins, K.D., Lical, J., and Ottemann, K.M. (2014). Internal Sense of Direction: Sensing and Signaling from Cytoplasmic Chemoreceptors. *Microbiol. Mol. Biol. Rev.* 78, 672–684.
- Collins, K.D., Andermann, T.M., Draper, J., Sanders, L., Williams, S.M., Araghi, C., and Ottemann, K.M. (2016). The *Helicobacter pylori* CZB Cytoplasmic Chemoreceptor TlpD Forms an Autonomous Polar Chemotaxis Signaling Complex That Mediates a Tactic Response to Oxidative Stress. *J. Bacteriol.* 198, 1563–1575.
- Curtis, P.D., and Brun, Y.V. (2010). Getting in the Loop: Regulation of Development in *Caulobacter crescentus*. *Microbiol. Mol. Biol. Rev.* 74, 13–41.
- Etesami, H. (2018). Bacterial mediated alleviation of heavy metal stress and decreased accumulation of metals in plant tissues: Mechanisms and future prospects. *Ecotoxicol. Environ. Saf.* 147, 175–191.

- Evinger, M., and Agabian, N. (1977). Envelope-Associated Nucleoid from *Caulobacter crescentus* Stalked and Swarmer Cells. *132*, 8.
- Ezraty, B., Gennaris, A., Barras, F., and Collet, J.-F. (2017). Oxidative stress, protein damage and repair in bacteria. *Nat. Rev. Microbiol.* *15*, 385–396.
- Freedman, J.H., Ciriolo, M.R., and Peisach, J. (1989). The Role of Glutathione in Copper Metabolism and Toxicity. *J. Biol. Chem.* *264*, 5598–5605.
- Gardès-Albert, M., Bonnefont-Rousselot, D., and Abedinzadeh, Z. (2003). Espèces réactives de l'oxygène. *Actual. Chim.* *91*.
- Goemans, C.V., Beaufay, F., Wahni, K., Van Molle, I., Messens, J., and Collet, J.-F. (2018). An essential thioredoxin is involved in the control of the cell cycle in the bacterium *Caulobacter crescentus*. *J. Biol. Chem.* *293*, 3839–3848.
- Gómez-Sagasti, M.T., Becerril, J.M., Martín, I., Epelde, L., and Garbisu, C. (2014). cDNA microarray assessment of early gene expression profiles in *Escherichia coli* cells exposed to a mixture of heavy metals. *Cell Biol. Toxicol.* *30*, 207–232.
- González, A.G., Shirokova, L.S., Pokrovsky, O.S., Emnova, E.E., Martínez, R.E., Santana-Casiano, J.M., González-Dávila, M., and Pokrovski, G.S. (2010). Adsorption of copper on *Pseudomonas aureofaciens*: Protective role of surface exopolysaccharides. *J. Colloid Interface Sci.* *350*, 305–314.
- H. Irving, and R. J. P. Williams (1953). The stability of transition-metal complexes. *J. Chem. Soc.* 3192–3210.
- Hassan, H.M., and Fridovich, I. (1979). Paraquat and *Escherichia coli*. Mechanism of production of extracellular superoxide radical. *J. Biol. Chem.* *254*, 10846–10852.
- Hazelbauer, G.L., Falke, J.J., and Parkinson, J.S. (2008). Bacterial chemoreceptors: high-performance signaling in networked arrays. *Trends Biochem. Sci.* *33*, 9–19.
- Hiniker, A., Collet, J.-F., and Bardwell, J.C.A. (2005). Copper Stress Causes an *in Vivo* Requirement for the *Escherichia coli* Disulfide Isomerase DsbC. *J. Biol. Chem.* *280*, 33785–33791.
- Hobman, J.L., and Crossman, L.C. (2015). Bacterial antimicrobial metal ion resistance. *J. Med. Microbiol.* *64*, 471–497.
- Hu, P., Brodie, E.L., Suzuki, Y., McAdams, H.H., and Andersen, G.L. (2005). Whole-Genome Transcriptional Analysis of Heavy Metal Stresses in *Caulobacter crescentus*. *J. Bacteriol.* *187*, 8437–8449.
- Italiani, V.C.S., da Silva Neto, J.F., Braz, V.S., and Marques, M.V. (2011). Regulation of Catalase-Peroxidase KatG Is OxyR Dependent and Fur Independent in *Caulobacter crescentus*. *J. Bacteriol.* *193*, 1734–1744.
- Johnson, K.S., and Ottemann, K.M. (2018). Colonization, localization, and inflammation: the roles of *H. pylori* chemotaxis in vivo. *Curr. Opin. Microbiol.* *41*, 51–57.

- Jones, C.W., and Armitage, J.P. (2015). Positioning of bacterial chemoreceptors. *Trends Microbiol.* *23*, 247–256.
- Kenney, G.E., and Rosenzweig, A.C. (2018). Chalkophores. *Annu. Rev. Biochem.* *87*, 645–676.
- Kim, E.-H., Nies, D.H., McEvoy, M.M., and Rensing, C. (2011). Switch or Funnel: How RND-Type Transport Systems Control Periplasmic Metal Homeostasis. *J. Bacteriol.* *193*, 2381–2387.
- Lacal, J., García-Fontana, C., Muñoz-Martínez, F., Ramos, J.-L., and Krell, T. (2010). Sensing of environmental signals: classification of chemoreceptors according to the size of their ligand binding regions: Chemoreceptor diversity. *Environ. Microbiol.* *12*, 2873–2884.
- Ladomersky, E., and Petris, M.J. (2015). Copper tolerance and virulence in bacteria. *Metallomics* *7*, 957–964.
- Lawarée, E., Gillet, S., Louis, G., Tilquin, F., Le Blastier, S., Cambier, P., and Matroule, J.-Y. (2016). *Caulobacter crescentus* intrinsic dimorphism provides a prompt bimodal response to copper stress. *Nat. Microbiol.* *1*, 16098.
- Leadem, L., Silva, L.G., Ribeiro, R.A., dos Santos, N.M., Lorenzetti, A.P.R., Alegria, T.G.P., Schulz, M.L., Medeiros, M.H.G., Koide, T., and Marques, M.V. (2018). Iron Deficiency Generates Oxidative Stress and Activation of the SOS Response in *Caulobacter crescentus*. *Front. Microbiol.* *9*.
- Lei, K., Sun, M., Du, L., Zhang, X., Yu, H., Wang, S., Hayat, T., and Alsaedi, A. (2017). Sensitive determination of endogenous hydroxyl radical in live cell by a BODIPY based fluorescent probe. *Talanta* *170*, 314–321.
- Liu, Y., Bauer, S.C., and Imlay, J.A. (2011). The YaaA Protein of the *Escherichia coli* OxyR Regulon Lessens Hydrogen Peroxide Toxicity by Diminishing the Amount of Intracellular Unincorporated Iron. *J. Bacteriol.* *193*, 2186–2196.
- Lu, D., Zhou, L., Wang, R., Zhang, X.-B., He, L., Zhang, J., Hu, X., and Tan, W. (2017). A two-photon fluorescent probe for endogenous superoxide anion radical detection and imaging in living cells and tissues. *Sens. Actuators B Chem.* *250*, 259–266.
- Lukyanov, K.A., and Belousov, V.V. (2014). Genetically encoded fluorescent redox sensors. *Biochim. Biophys. Acta BBA - Gen. Subj.* *1840*, 745–756.
- Macomber, L., and Imlay, J.A. (2009). The iron-sulfur clusters of dehydratases are primary intracellular targets of copper toxicity. *Proc. Natl. Acad. Sci.* *106*, 8344–8349.
- Macomber, L., Rensing, C., and Imlay, J.A. (2007). Intracellular Copper Does Not Catalyze the Formation of Oxidative DNA Damage in *Escherichia coli*. *J. Bacteriol.* *189*, 1616–1626.
- Morse, M., Colin, R., Wilson, L.G., and Tang, J.X. (2016). The Aerotactic Response of *Caulobacter crescentus*. *Biophys. J.* *110*, 2076–2084.
- Narayanan, S., Janakiraman, B., Kumar, L., and Radhakrishnan, S.K. (2015). A cell cycle-controlled redox switch regulates the topoisomerase IV activity. *Genes Dev.* *29*, 1175–1187.

- Nesper, J., Hug, I., Kato, S., Hee, C.-S., Habazettl, J.M., Manfredi, P., Grzesiek, S., Schirmer, T., Emonet, T., and Jenal, U. (2017). Cyclic di-GMP differentially tunes a bacterial flagellar motor through a novel class of CheY-like regulators. *ELife* 6.
- Nies, D.H., and Herzberg, M. (2013). A fresh view of the cell biology of copper in enterobacteria: Cell biology of copper in enterobacteria. *Mol. Microbiol.* 87, 447–454.
- Njuma, O.J., Ndontsa, E.N., and Goodwin, D.C. (2014). Catalase in peroxidase clothing: Interdependent cooperation of two cofactors in the catalytic versatility of KatG. *Arch. Biochem. Biophys.* 544, 27–39.
- Ortega, Á., Zhulin, I.B., and Krell, T. (2017). Sensory Repertoire of Bacterial Chemoreceptors. *Microbiol. Mol. Biol. Rev.* 81.
- Østergaard, H., Tachibana, C., and Winther, J.R. (2004). Monitoring disulfide bond formation in the eukaryotic cytosol. *J. Cell Biol.* 166, 337–345.
- Paintdakhi, A., Parry, B., Campos, M., Irnov, I., Elf, J., Surovtsev, I., and Jacobs-Wagner, C. (2016). Oufiti: an integrated software package for high-accuracy, high-throughput quantitative microscopy analysis: Oufiti: image analysis software. *Mol. Microbiol.* 99, 767–777.
- Parkinson, J.S., Hazelbauer, G.L., and Falke, J.J. (2015). Signaling and sensory adaptation in *Escherichia coli* chemoreceptors: 2015 update. *Trends Microbiol.* 23, 257–266.
- Salah Ud-Din, A.I.M., and Roujeinikova, A. (2017). Methyl-accepting chemotaxis proteins: a core sensing element in prokaryotes and archaea. *Cell. Mol. Life Sci.* 74, 3293–3303.
- Schnell, S., and Steinman, H.M. (1995). Function and stationary-phase induction of periplasmic copper-zinc superoxide dismutase and catalase/peroxidase in *Caulobacter crescentus*. *J. Bacteriol.* 177, 5924–5929.
- Sies, H. (2015). Oxidative stress: a concept in redox biology and medicine. *Redox Biol.* 4, 180–183.
- Sies, H., Berndt, C., and Jones, D.P. (2017). Oxidative Stress. *Annu. Rev. Biochem.* 86, 715–748.
- Solioz, M. (2018). *Copper and Bacteria: Evolution, Homeostasis and Toxicity* (Cham: Springer International Publishing).
- Steinman, H.M. (1993). Function of periplasmic copper-zinc superoxide dismutase in *Caulobacter crescentus*. *J. Bacteriol.* 175, 1198–1202.
- Steinman, H.M., Fareed, F., and Weinstein, L. (1997). Catalase-peroxidase of *Caulobacter crescentus*: function and role in stationary-phase survival. *J. Bacteriol.* 179, 6831–6836.
- Taktikos, J., Stark, H., and Zaburdaev, V. (2013). How the Motility Pattern of Bacteria Affects Their Dispersal and Chemotaxis. *PLoS ONE* 8, e81936.
- Wadhams, G.H., and Armitage, J.P. (2004). Making sense of it all: bacterial chemotaxis. *Nat. Rev. Mol. Cell Biol.* 5, 1024–1037.

Zhou, P., Zhang, J., Zhang, Y., Liu, Y., Liang, J., Liu, B., and Zhang, W. (2016). Generation of hydrogen peroxide and hydroxyl radical resulting from oxygen-dependent oxidation of l - ascorbic acid via copper redox-catalyzed reactions. *RSC Adv.* 6, 38541–38547.